Available online at www.sciencedirect.com

SCIENCE DIRECT®

Lithos 80 (2005) 1–32

LITHOS

www.elsevier.com/locate/lithos

# Comparison of Proterozoic and Phanerozoic rift-related basaltic-granitic magmatism

Ilmari Haapala*, O. Tapani Rämö, Stephen Frindt[1]

*Department of Geology, P.O. Box 64, FI-00014, University of Helsinki, Finland*

Received 9 June 2003; accepted 9 September 2004
Available online 11 November 2004

**Abstract**

This paper compares the 1.67–1.47 Ga rapakivi granites of Finland and vicinity to the 1.70–1.68 Ga rapakivi granites of the Beijing area in China, the anorogenic ~130 Ma granites of western Namibia, and the 20–15 Ma granites of the Colorado River extensional corridor in the Basin and Range Province of southern Nevada. In Finland and China, the tectonic setting was incipient, aborted rifting of Paleoproterozoic or Archean continental crust, in Namibia it was continental rifting and mantle plume activity that led to the opening of southern Atlantic at ~130 Ma. The 20–15 Ma granites of southern Nevada were related to rifting that followed the Triassic–Paleogene subduction of the Farallon plate beneath the southwestern United States. In all cases, extension-related magmatism was bimodal and accompanied by swarms of diabase and rhyolite–quartz latite dikes. Rapakivi texture with plagioclase-mantled alkali feldspar megacrysts occurs in varying amounts in the granites, and the latest intrusive phases are commonly topaz-bearing granites or rhyolites that may host tin, tungsten, and beryllium mineralization. The granites are typically ferroan alkali-calcic metaluminous to slightly peraluminous rocks with A-type and within-plate geochemical and mineralogical characteristics. Isotope studies (Nd, Sr) suggest dominant crustal sources for the granites. The preferred genetic model is magmatic underplating involving dehydration melting of intermediate-felsic deep crust. Juvenile mafic magma was incorporated either via magma mingling and mixing, or by remelting of newly hybridized lower crust. In Namibia, partial melting of subcontinental lithospheric mantle was caused by the Tristan mantle plume, in the other cases the origin of the mantle magmatism is controversial. For the Fennoscandian suites, extensive long-time mantle upwelling associated with periodic, migrating melting of the subcontinental lithospheric mantle, governed by heat flow and deep crustal structures, is suggested.
© 2004 Elsevier B.V. All rights reserved.

*Keywords:* A-type granite; Bimodal association; Rifting; Diabase; Rapakivi granite

## 1. Introduction

Continental rifting and resultant faulting, rapid erosion, and deposition of clastic sediments, as well as volcanic and plutonic activity are in several cases

* Corresponding author. Tel.: +358 9 590400; fax: +358 9 19150826.
*E-mail address:* ilmari.haapala@helsinki.fi (I. Haapala).
[1] Present address: Geological Survey of Namibia, P.O. Box 2168, 1 Aviation Rd., Windhoek, Namibia.

0024-4937/$ - see front matter © 2004 Elsevier B.V. All rights reserved.
doi:10.1016/j.lithos.2004.04.057

associated with hot mantle plumes. Rifting may vary from incipient (aborted) with only minor extension to the break-up of continents and opening of oceans (e.g., White and McKenzie, 1989; Windley, 1995, pp. 51–64, 98–104, 262–276; Peccerillo et al., 2003). The nature of the associated magmatism varies from alkaline to subalkaline, and bimodal suites are typical of most continental rifting environments.

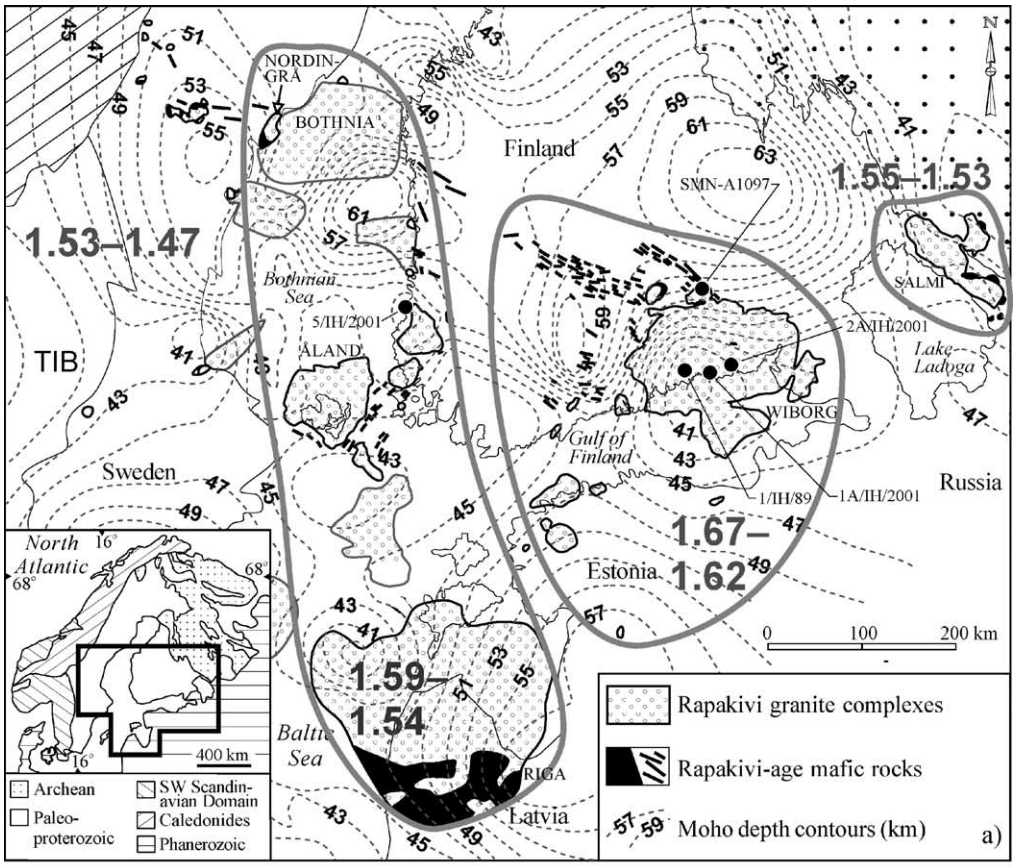
This paper summarizes the results of studies led by the Department of Geology, University of Helsinki, on rapakivi-type granites and related mafic rocks associated with continental rifting in Finland, China, Namibia, and the western United States. The main aim of these studies has been to test whether the magmatic underplate model (see Bridgewater et al., 1974; Emslie, 1978), first applied to the Finnish rapakivi granites by Haapala (1985) and Haapala and Rämö (1990), is applicable to the rapakivi granites and related rocks of the other regions. The study areas were chosen to supplement each other and give as comprehensive information as possible on the tectonic setting, magmatic association, granite-related mineralization, and petrogenesis of the igneous suites. Southern Finland, the classic rapakivi area with 1.67–1.54 Ga rapakivi granites and associated diabase and quartz-porphyritic dike swarms enclosed in a 1.9 Ga cratonized crust, is taken as the reference area. The 1.7 Ga Shachang rapakivi granite complex near Beijing, China was emplaced, together with diabase dikes, in Neoarchean cratonized crust. In northwestern Namibia, Cretaceous granites resembling evolved rapakivi granites intruded, together with mafic and felsic dikes, into the cratonized Neoproterozoic–Paleozoic Damara orogenic crust. They were related to mantle plume activity and rifting which led to the opening of the South Atlantic. Miocene granites and associated diabase and rhyolite dikes of southernmost Nevada, Basin and Range Province, represent a modern example of an extensional environment with rapakivi-type magmatism. The studies have included field mapping as well as petrographic, geochronological, and geochemical (including isotopic) studies.

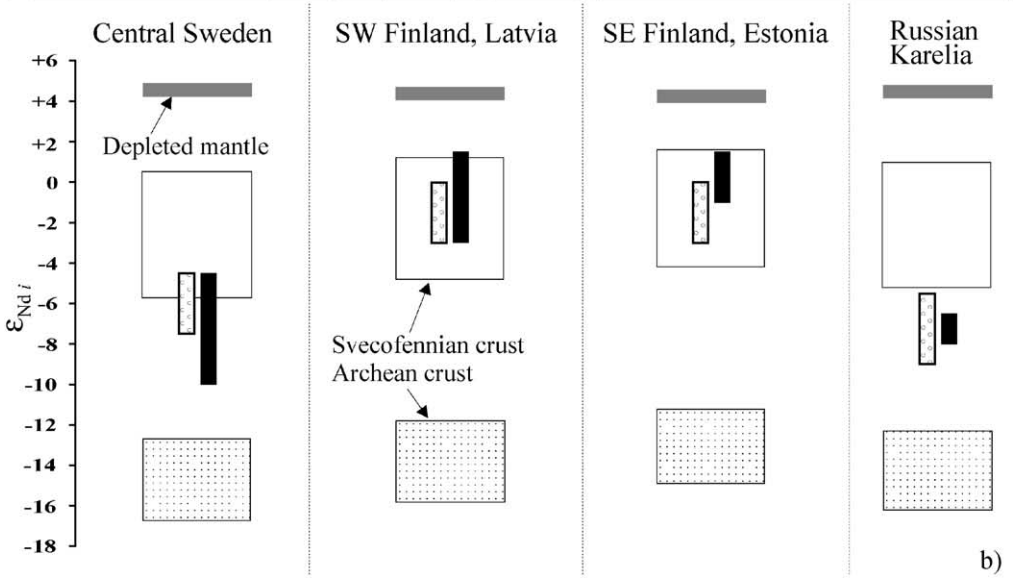
## 2. The 1.67–1.47 Ga rapakivi granites of Finland and vicinity

### 2.1. Geologic setting

The major Precambrian tectonic units of Fennoscandia comprise (1) the Archean 3.1–2.6 Ga granite gneiss–greenstone belt domain in the east, (2) the broad 1.9–1.8 Ga Svecofennian orogenic belt, and (3) the 1.7–1.5 Ga Gothian or Southwest Scandinavian domain in the southwest (see Fig. 1 inset). Major cratonic magmatic events are represented by 2.45 Ga layered mafic intrusions and associated granitoids in northern Finland (Alapieti, 1982; Rämö and Luukkonen, 2001; Lauri and Mänttäri, 2002) and the 1.67–1.47 Ga rapakivi granites and associated mafic rocks (diabase dikes, gabbros, anorthosites). Current syntheses of the evolution of the Fennoscandian lithosphere can be found in Nironen (1997), Korsman et al. (1999), and Pesonen et al. (2000). These studies utilized also extensive geophysical data including deep seismic soundings. As currently perceived, the Svecofennian crust was formed by complex accretion of island arcs and microcontinents from west and south to the Archean craton at 1.92–1.88 Ga. Subsequent thickening of the crust and remelting were related to magmatic underplating at 1.89–1.87 Ga (Korsman et al., 1999; Nironen et al., 2000). Collision-related melting of the felsic sedimentary-volcanic complex of southern Finland and central Sweden at 1.84–1.80 Ga produced a belt of migmatite-related potassic S-type granites. Emplacement of post-collisional shoshonitic and granitic plutons at ~1.80 Ga completed the Svecofennian orogenic evolution (Nironen, 1997; Eklund et al., 1998; Korsman et al., 1999).

Fig. 1. (a) Map showing the distribution and ages of the rapakivi granite complexes and diabase dikes as well as contours of crustal thickness in the south-central part of the Fennoscandian shield. The subvertical lines outline four rapakivi age zones (1.53–1.47, 1.59–1.54, 1.67–1.62, and 1.55–1.54 Ga). Sites for the five representative samples (Table 1) are indicated. The inset shows the area in relation to the major crustal domains in the shield. TIG is the Transcandinavian Igneous Belt. The map is from Rämö and Korja (2000) and Rämö et al. (2000), where the pertinent references are given. (b) Diagram showing variation of initial Nd isotope composition ($\varepsilon_{Ndi}$) in the rapakivi granites (open-circle pattern) and related mafic-intermediate rocks (black) in the four age zones. The composition of the depleted mantle (DePaolo, 1981), the ~1.9 Ga Svecofennian rocks (Huhma, 1986; Patchett and Kouvo, 1986), and the Archean crust of the Fennoscandian shield (Rämö et al., 1996) are shown at the time of interest. Adopted from Rämö et al. (2000), where also a more comprehensive list of references is given.


NORDIN-GRÅ
BOTHNIA
Finland
SMN-A1097
1.55–1.53
1.53–1.47
Bothnian Sea
5/IH/2001
ÅLAND
TIB
SALMI
2A/IH/2001
Lake Ladoga
WIBORG
Gulf of Finland
Sweden
Russia
1/IH/89
1A/IH/2001
1.67–1.62
Estonia
North Atlantic
400 km
1.59–1.54
Baltic Sea
RIGA
Latvia
0 100 200 km
N
Archean
Paleo-proterozoic
SW Scandin-avian Domain
Caledonides
Phanerozoic
Rapakivi granite complexes
Rapakivi-age mafic rocks
Moho depth contours (km)
a)


Central Sweden
SW Finland, Latvia
SE Finland, Estonia
Russian Karelia
Depleted mantle
Svecofennian crust
Archean crust
εNd i
+6
+4
+2
0
-2
-4
-6
-8
-10
-12
-14
-16
-18
b)

### 2.2. Mode of occurrence

The 1.65–1.47 Ga rapakivi granites are found as epizonal composite batholiths and stocks in the Proterozoic Svecofennian crust (Fig. 1). The Salmi batholith in the east is, however, located mainly in Archean rocks at the border between the exposed Archean craton and the Proterozoic crust. The two largest batholiths, Riga and Wiborg, measure (without satellitic intrusions) 40,600 and 18,500 km$^2$, respectively. Deep seismic soundings and gravity studies indicate that even the large batholiths are subhorizontal sheets with thicknesses of about 5–10 km. The magmatic association is bimodal. The felsic members are represented by several different types of granite, quartz porphyry dikes, and rare extrusive equivalents, the mafic members by tholeiitic diabase dikes, gabbroids, anorthosites, and local monzodiorites. Mingling and mixing between the mafic and felsic magmas is evident in several localities (e.g., Rämö, 1991; Eklund et al., 1994; Salonsaari, 1995; Alviola et al., 1999). Some examples of the mingling-mixing structures and textures from Finland and other study areas of this paper are presented in Fig. 2.

### 2.3. Age distribution and tectonic setting

U–Pb geochronology shows that the rapakivi granites and associated diabase and quartz porphyry dikes of the Fennoscandian shield can be divided into four area-constrained age groups (Vaasjoki et al., 1991; Rämö, 1991; Suominen, 1991; Neymark et al., 1994; Rämö et al., 1996; Lindh and Johansson, 1996; Andersson, 1997; Claesson and Kresten, 1997; Ahl et al., 1997; Alviola et al., 1999; Persson, 1999; Andersson et al., 2002): the Salmi batholith is 1.56–1.53 Ga; the Wiborg batholith and its satellites in Finland and Estonia as well as the extensive WNW-trending diabase (and associated quartz porphyry) dikes in Finland are 1.67–1.62 Ga; the Riga, Åland, Vehmaa, Laitila, Nordingrå, and Bothnia batholiths and the NNE-trending diabase dikes in southwestern Finland are 1.59–1.54 Ga; and the rapakivi complexes and associated dikes in central Sweden 1.53–1.47 Ga (Fig. 1). The oldest rapakivi granites and diabase dikes are thus located in the central part of the province. The 1.59–1.54 Ga rapakivi complexes and associated graben structures appear to form a 200- to 250-km-wide and at least 800-km-long N-trending zone that extends from Latvia (Riga batholith) along the Gulf of Bothnia to the Bothnia batholith. This zone has been interpreted as an aborted paleorift within a broad (about 800 by 800 km) rifted area extending from Lake Ladoga in the east to the Caledonides in the west (Korja et al., 2001). Some ENE- and ~N-trending diabase dikes along the western coast of Finland follow this zone. The other age groups do not form clear belts, and the 1.67–1.62 and 1.56–1.53 Ga age groups can best be depicted as rounded subprovinces (see Puura and Flodén, 1999).

Extensional tectonic setting of the rapakivi magmatism is indicated by the extensive swarms of mainly WNW-trending (in southwestern Finland ENE-trending) diabase and rhyolitic porphyry dikes (Fig. 1), faults and NW-trending graben structures (Haapala, 1985; Haapala and Rämö, 1992), and subsurface listric faults (Korja and Heikkinen, 1995; Rämö and Korja, 2000; Korja et al., 2001). The marked thinning of the crust—especially the lower crust—in areas of rapakivi granites (Figs. 1 and 4a; Luosto et al., 1990; Luosto, 1997; Korja et al., 1993) is probably in part related to regional extension, but the subcircular shape of the mantle domes and overlying thinned crust suggest that local mantle upwelling and related extensive melting of the lower crust were also important (see Haapala and Rämö, 1992; Rämö and Haapala, 1996; Korja et al., 2001). The lower crust has P wave velocities between 7 and 7.7 km/s (in Fig. 4, 7 to 7.3 km/s). In the apical parts of the mantle domes, there is a transitional zone (in Fig. 4, velocities 8 to 8.2 km/s), which is supposed to consist of mantle peridotite and intruded gabbroic rocks. In the Moho depth maps (e.g., Korja et al., 1993; Luosto, 1997) and in Figs. 1 and 4a, the transitional zone is regarded as part of the uppermost mantle.

Unlike the rapakivi granites, the diabase dikes are not restricted to areas of thinner crust, and the Häme and Suomenniemi dike swarms northwest and north of the Wiborg batholith (Fig. 1a) transect the thick Svecofennian crust of central Finland. The change in the direction of the diabase dike swarms from one age group to another (e.g., the 1.67–1.62 and 1.59–1.54 Ga groups) indicates that the effective strain pattern changed temporally or laterally. Evidence of advanced rifting is, however, missing.

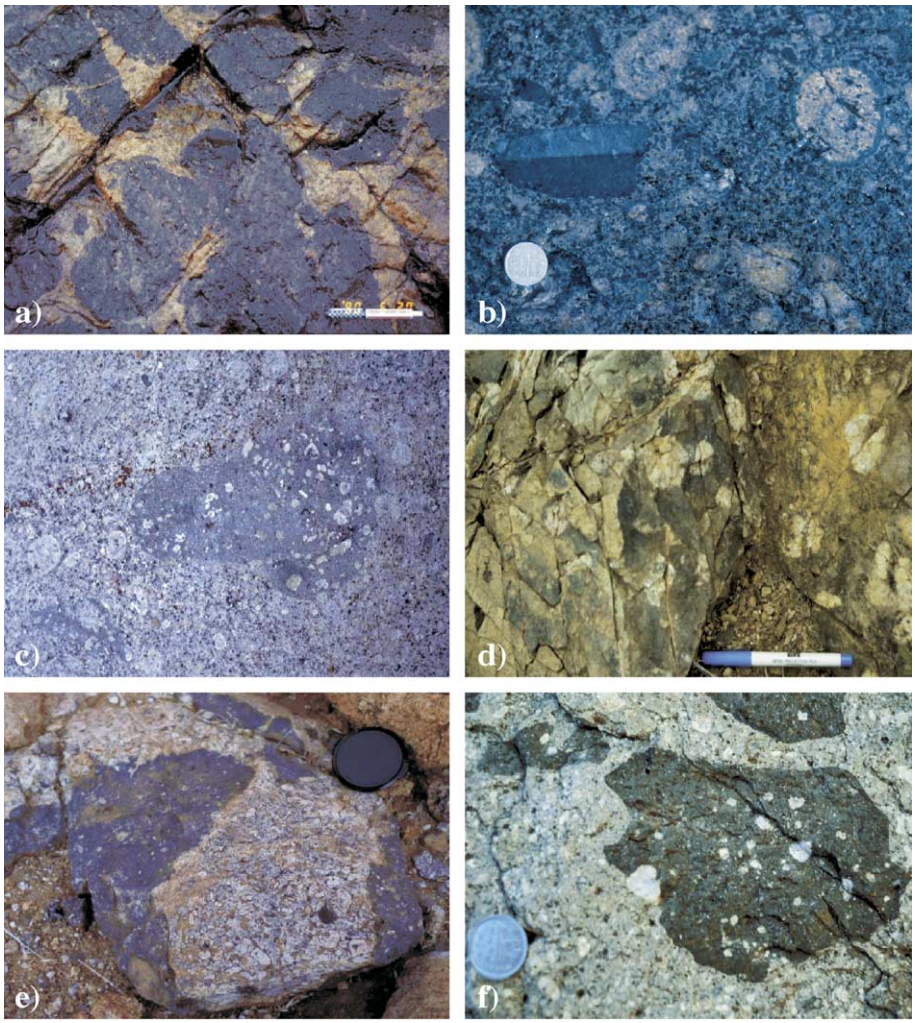



Fig. 2. Structures and textures related to the interaction (mingling and mixing) of coexisting mafic and felsic magmas in the bimodal magmatic suites of this study. (a) Pillows of monzodiorite in granite from the Ahvenisto rapakivi complex, southeastern Finland (Alviola et al., 1999). (b) Dark labradorite xenocryst (left) and andesine–oligoclase-mantled alkali feldspar ovoids in dark wiborgite on the Ristisaari Island in the southwestern part of the Wiborg batholith. (c) A dark hybrid enclave containing more mafic "enclaves in enclave" as well as alkali feldspar and quartz xenocrysts in a hybrid hornblende-bearing granite of the Jaala-Iitti complex, southeastern Finland (Salonsaari, 1995). (d) Alkali feldspar xenocrysts in a diabase dike cutting the biotite–hornblende granite of the Shachang pluton, China. (e) Comingled mafic pillows in the porphyritic granite at the northeastern margin of the Gross Spitzkoppe stock, Namibia (Frindt, 2002). In this case, close to the mafic pillows, the topaz-bearing granite has alkali feldspar megacrysts mantled by plagioclase (rapakivi texture sensu lato). (f) Mafic enclaves with alkali feldspar and quartz xenocrysts in rhyolite from a composite dike that cuts the Spirit Mountain granite in southernmost Nevada. Many of the alkali feldspar megacrysts in enclaves and rhyolite have plagioclase–quartz shells. Photos: (a), (c)–(f) Ilmari Haapala; (b) Tapani Rämö.

### 2.4. Petrography and geochemistry

The rapakivi granite batholiths and stocks are usually composed of several petrographically distinct granite types, and in some cases minor gabbroic, anorthositic, monzodioritic and syenitic bodies are also found (e.g., Vorma, 1976; Rämö, 1991; Alviola et al., 1999). The earlier granite phases are commonly hornblende–biotite (±fayalite) granites, followed by biotite granites and less common topaz-bearing alkali feldspar granites. The wiborgitic rapakivi granites with plagioclase-mantled alkali

feldspar megacrysts are hornblende bearing. Greisen-type Sn–Be–W–Zn mineralization is associated with the topaz-bearing granites (Haapala, 1977a, 1995, 1997; Edén, 1991).

In geochemical and mineral chemical composition, the rapakivi granites are typical aluminous A-type granites (cf. King et al., 1997). Especial characteristics are high K, Fe/Mg, F, Ga, Rb, and Zr (except in the topaz-bearing granites) (e.g., Vorma, 1976; Haapala, 1977b; Rämö, 1991). The Fe/(Fe+Mg) number in biotite varies from 0.80 to 1.00 (Rieder et al., 1996), and in hornblende from 0.77 to 0.95 (Simonen and Vorma, 1969). In various differentiation diagrams, the granites plot into the A-type fields of Whalen et al. (1987) and within-plate granite fields of Pearce et al. (1984) (Fig. 3a, b). The multielement diagram (Fig. 3c), with strong enrichments in Th and U and depletion in Sr, is typical of A-type granites (e.g., Whalen et al., 1996). The REE patterns (Fig. 3d) show enrichment in the LREEs and negative Eu anomalies. With increasing magmatic fractionation, the enrichment in LREE decreases and the Eu anomaly deepens. The fayalite–magnetite–quartz association in the more mafic rapakivi granites and the common prevalence of ilmenite over magnetite indicate reducing conditions (ilmenite series of Ishihara, 1977).

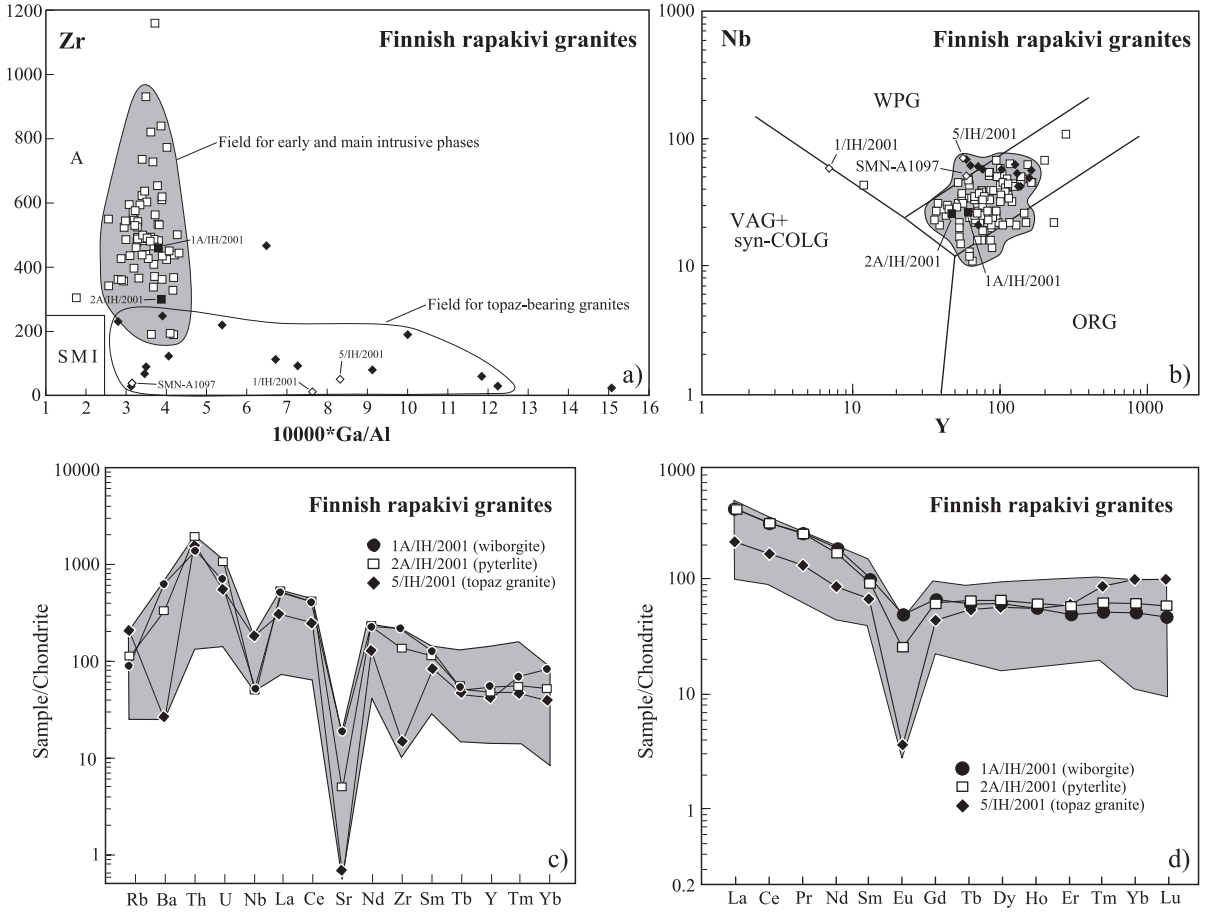



Fig. 3. Analyses of Finnish rapakivi granites plotted in (a) Zr versus 10,000 Ga/Al (Whalen et al., 1987), (b) Nb versus Y (Pearce et al., 1984), (c) a chondrite-normalized multielement, and (d) a chondrite-normalized REE diagrams (overall fields and type analyses marked). Data from Vorma (1976), Haapala (1977a,b), Rämö (1991), Lindberg and Bergman (1993), Salonsaari (1995), Rieder et al. (1996), Kosunen (1999), and Table 1.

### 2.5. Isotope geochemistry and petrogenesis

Since 1990, large amounts of new U–Pb, Nd, common Pb, and Sr isotope data have been published on the rapakivi complexes of Fennoscandia (Haapala and Rämö, 1990; Rämö, 1991, 2001; Vaasjoki et al., 1991; Neymark et al., 1994; Rämö et al., 1996; Amelin et al., 1997; Claesson and Kresten, 1997; Andersson, 1997; Persson, 1999; Alviola et al., 1999; Lindh, 2001; Andersson et al., 2002). The Sm–Nd system has proven to be an especially useful indicator of the overall age and nature of the sources of the rapakivi granites. Some results are summarized in Figs. 1 and 7.

The rapakivi granites of Finland have initial $\varepsilon_{Nd}$ values between −3 and 0, suggesting derivation from the 1.9 Ga Svecofennian crust (Haapala and Rämö, 1990; Rämö, 1991). The Salmi rapakivi batholith, located at the Archean–Proterozoic boundary in Russian Karelia, shows more negative $\varepsilon_{Nd}$ values of −9 to −5.5, suggesting that a major Archean source component mixed with Svecofennian or younger, rapakivi-age component (Rämö, 1991; Neymark et al., 1994). The rapakivi granites of central Sweden have also strongly negative $\varepsilon_{Nd}$ values of −7.5 to −4.5, implying the presence of an Archean basement underneath the exposed Svecofennian crust (Andersson, 1997; Andersson et al., 2002). The clastic metasediments of the Svecofennian Bothnian Basin in central Sweden have $\varepsilon_{Nd}$ (at 1.51 Ga) values (−10.2 to −5.8) that overlap those of the rapakivi granites (Welin et al., 1993; Andersson et al., 2002).

The mafic rocks (diabase dikes, gabbroids) have $\varepsilon_{Nd}$ values that largely overlap with those of the associated rapakivi granites (Figs. 1 and 7). However, the diabase dikes of the Suomenniemi and Häme swarms (Wiborg rapakivi area) show $\varepsilon_{Nd}$ values that are higher (up to +1.6) than those of the associated rapakivi granites. The mafic and hybrid intermediate rocks of central Sweden have low $\varepsilon_{Nd}$ (at 1.51 Ma) values (−8.9 to −6.5), some of which are more negative than those of the rapakivi granites (Andersson et al., 2002). In the Salmi batholith of Russian Karelia, the $\varepsilon_{Nd}$ values of the mafic and intermediate rocks (−6.5 to −7.5) overlap with those of the granites (Neymark et al., 1994).

The isotopic overlap of the mafic and felsic members of the rapakivi suites could suggest that the felsic magmas were formed by fractional crystallization of mantle-derived mafic parental magmas (see discussion in Frost et al., 2002). This is, however, regarded unlikely because granitic rocks generally greatly prevail over mafic and intermediate rocks in the rapakivi complexes. Numerous observations of mingling structures and textures indicate simultaneous presence of mafic and felsic magmas (Rämö, 1991; Eklund et al., 1994; Salonsaari, 1995). Further, the thinning of the lower crust above mantle domes and the transitional zones (Fig. 4b) is compatible with the interpretation that rapakivi magmas are of deep crustal origin rather than mantle fractionates. Therefore, different main sources, mantle and crust, are preferred for the mafic and felsic magmas, respectively.

Rämö (1991) suggested that the rapakivi granites of Finland (the Suomenniemi batholith) were originated by about 20% partial melting of intermediate-felsic (tonalitic-granodioritic) Svecofennian lower crust; for the rapakivis of the Salmi batholith, a mixed (Archean–Svecofennian) source was invoked. Kosunen et al. (2004) proposed that the parent magmas of the Obbnäs rapakivi granites in southern Finland originated by partial melting of ferrodioritic/ferromonzodioritic or tonalitic source, with contribution through mixing from a juvenile mafic (diabase) melt, whereas the adjacent Bodom granite had a granodioritic source. Kosunen et al. (2004) concluded that stepwise fractionation of tholeiitic basalt is an unlikely process for producing the trace element distribution of the granites. For the rapakivi granites of central Sweden, Andersson et al. (2002) preferred a mixed source composed of dominantly Svecofennian and 30–40% Archean metaigneous rocks.

Neymark et al. (1994) suggested an interesting model for the rocks of the Salmi batholith. This involves Svecofennian magmatic underplating with interaction between the mantle-derived magmas and the Archean crust, which led to the formation of a hybrid, melt-depleted lower crust. When the mafic residues of these melting and differentiation processes returned to the mantle, carrying with them material from the lower continental crust, a zone of hybrid uppermost mantle was formed. Both the hybrid zones had mixed isotopic character. Subsequent mantle upwelling caused partial melting of the lower crust and formation of the rapakivi granite magmas, whereas partial melting of the enriched upper mantle

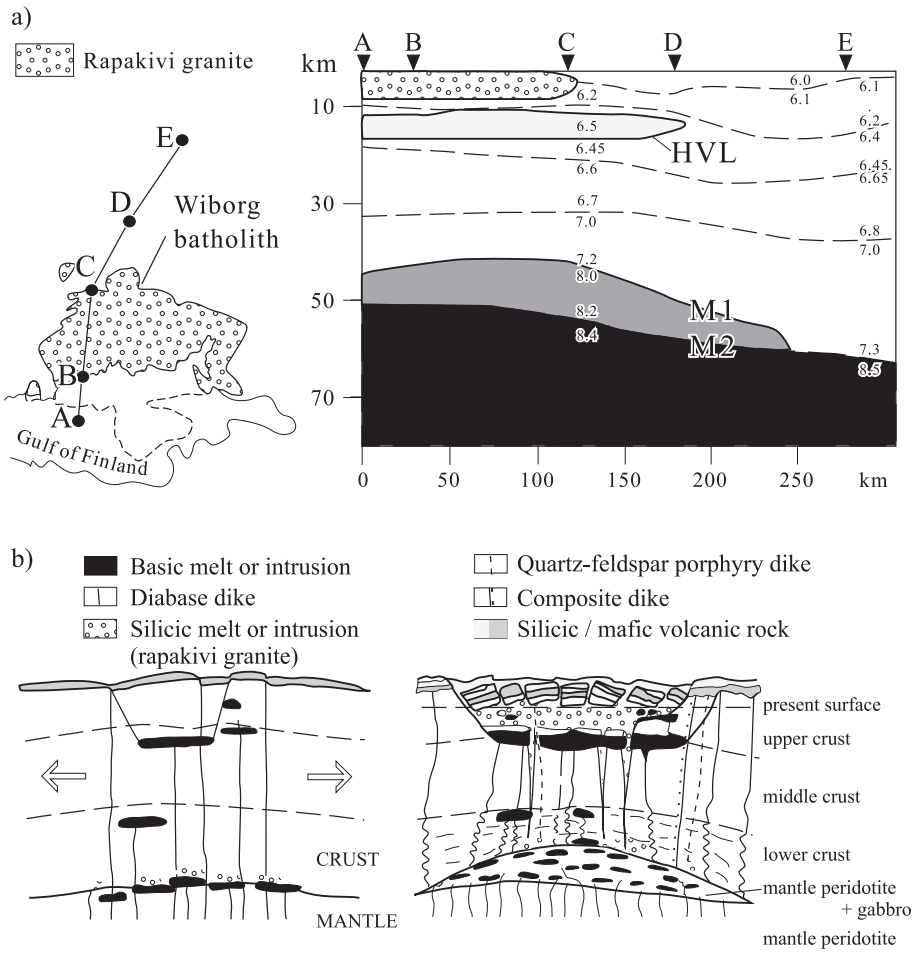



Fig. 4. (a) A vertical section across the Wiborg rapakivi granite batholith showing the structure of the crust and upper mantle according to Luosto et al. (1990) and Korja et al. (1993). The broken lines show changes in P wave velocities. HVL is a high-velocity layer (probably gabbroic rocks), and M1 and M2 mark a transitional zone at the crust–mantle boundary (from Rämö and Haapala, 1996). (b) A model for the origin of the bimodal rapakivi granite complexes of Finland according to Haapala (1989) and Rämö and Haapala (1996). Mantle-derived mafic magmas are intruded to the crust–mantle boundary, where they form a magmatic underplate, a hybrid of mantle peridotite, gabbro, and possible crustal material. Parts of the mafic magmas intrude to higher crustal levels producing gabbroic-anorthositic intrusions, diabase dikes, and basaltic lava fields. The magmatic underplate causes extensive partial melting of the lower crust producing A-type granitic magmas—parents of the rapakivi granites, quartz porphyry dikes, and rhyolitic volcanic rocks. Mingling and hybridization of the granitic and mafic magmas occurs locally in all crustal levels. Partial melting and transit of the granitic magmas to higher crustal levels, possibly coupled with extensional stretching, causes the thinning of the lower crust.

produced the parental magmas of the mafic rocks. This interpretation has similarities with the model of Emslie et al. (1994) for the Nain plutonic suite of Labrador. The model of Neymark et al. (1994) is supported by the discoveries of granulitic lower crustal xenoliths in a Devonian lamprophyre diatreme on Elovy island in southern Kola Peninsula (Kempton et al., 2001, and references therein) and in a 0.6 Ga kimberlite diatreme in Lahtojoki near Kuopio, eastern Finland, in the area of >58 km thick crust (Hölttä et al., 2000). The xenoliths are mainly mafic garnet-bearing granulites, with some intermediate-felsic granulites. It appears that below the Archean crust, close to the Paleoproterozoic (Svecofennian) domain, is a predominantly mafic lower crust, which shows petrographic and isotopic evidence of at least two

episodes of magmatism and reworking including K-metasomatism. U–Pb zircon age determinations of the lower crustal xenoliths suggest that in the Kola area the main magmatism and reworking episodes took place at 2.5–2.4 Ga (time of basaltic magmatism that produced the large layered mafic intrusions of the northern Fennoscandian shield) and at ~1.7 Ga (time of granitic magmatism in the upper crust) (Downes et al., 2002). For the lower crust of the Kuopio area (eastern Finland), U–Pb ages of zircon in xenoliths and zircon xenocrysts in the Lahtojoki kimberlite imply main growth and reworking episodes at 2.7 and 1.8 Ga (Hölttä et al., 2000; Peltonen and Mänttäri, 2001). The granulite xenoliths of Elovy island show a wide variation in isotopic composition; $\varepsilon_{Nd}$ (at 1.54 Ga) values vary from +6.8 to −11.1 (commonly from −5 to −9), covering the field of the Salmi rapakivi complex (Neymark et al., 1994; Kempton et al., 2001). Available three whole-rock Nd isotope analyses of the Lahtojoki xenoliths (Hölttä et al., 2000) give $\varepsilon_{Nd}$ (at 1.64 Ga) values of −3.5, −2.5, and +2.8, grossly matching the field of the granites of the Wiborg batholith. It is unlikely, however, that partial melting of this type of mafic lower crust could have produced the typical REE distribution of the rapakivi granites (see Elliott, 2003).

A problem with a metaigneous tonalitic-granodioritic source is that melting of such a source would generally produce high-$fO_2$ (magnetite-type) granites rather than reduced ilmenite-type rocks typical of the rapakivi association. Frost and Frost (1997) suggested melting of a tholeiitic mafic-intermediate igneous source for the formation of the reduced rapakivi granites of Wyoming. Taking into account the metaluminous-peraluminous character of the Fennoscandian rapakivi granites and the overlapping Nd isotope compositions of the Svecofennian metasediments and rapakivi granites of the same areas (e.g., Welin et al., 1993; Andersson et al., 2002), fusion of some metasedimentary rocks (metagreywackes) is also possible. In the Archean and early Paleoproterozoic, sediments and their derivatives would generally be in reduced state because of the common presence of biogenic carbon in the sedimentary rocks and the low oxygen content of the atmosphere (see Karhu and Holland, 1996). However, low boron contents of the rapakivi granites do not support any higher incorporation of sedimentary material.

The diabases, gabbros, and anorthosites of Finland and Estonia (age groups 1.67–1.62 and 1.59–1.54 Ga) with $\varepsilon_{Nd}$ +1.6 to −1.7 were obviously fractionated from mafic magmas that had been derived from a mantle source characterized by long-term LREE depletion, and were variously contaminated with crustal materials (Rämö, 1991). The origin of the mafic rocks of the Salmi batholith and central Sweden is more problematic. They may have been formed from mafic magmas generated by partial melting of LREE-enriched subcontinental lithospheric mantle, with little crustal assimilation (Neymark et al., 1994; Rämö et al., 2000), or from non-enriched mafic magmas that had assimilated and melted Archean/Svecofennian crustal rocks. The crustal assimilants may have been intermediate-felsic metaigneous rocks (Rämö, 1991; Andersson et al., 2002), mafic-intermediate metaigneous rocks formed by earlier (Svecofennian or later) magmatic underplatings (see Frost and Frost, 1997; Frost et al., 1999), or plagioclase–pyroxene granulite residue after extraction of granitic magmas (see Emslie et al., 1994). Advanced assimilation of plagioclase-rich granulite could help to explain the presence of anorthositic rocks in some rapakivi complexes.

The evidence for the source of the mafic and granitic magmas is not unequivocal. If the mantle-derived magmas were able to cause large-scale remelting of the lower crust, then also effective contamination with older crustal components and change in isotope composition of the mantle magmas would be expected. Processes involving low-degree remelting and assimilation of tholeiitic mafic-intermediate lower crust by mantle magmas could explain chemical characteristics of the mafic and felsic members of the bimodal association as well as the reduced (ilmenite-series) character of the rapakivi granites (see Frost and Frost, 1997; Frost et al., 1999). Another question is could such low-degree partial melting have produced the huge amount of granitic magma of the rapakivi batholiths of Fennoscandia and thinning of the lower crust below the rapakivi batholiths.

We think that the source of large rapakivi granite complexes of Fennoscandia did not consist of one rock type only, but comprised a suite of rocks, mainly intermediate-felsic but not necessarily only metaigneous rocks, that were fused successively and in varying amounts. The input of mantle magmas left its signatures also in the granites, either by hybridization

of felsic crustal magmas and mafic mantle-derived magmas (for which there is convincing field evidence), or by anatectic melting of crustal rocks hybridized in earlier (Svecofennian and/or later, rapakivi-age) magmatic underplating(s) (cf. Hildreth et al., 1991). The differences in the average chemical composition of the rapakivi complexes in southeast Fennoscandia (Vorma, 1976; Rämö and Haapala, 1995) probably reflect variations in the relative amounts of the fused source rocks, although also depth of erosion level may have caused significant differences in this respect. The overall source of the different plutons has probably varied from ferrodioritic to granodioritic in composition.

### 2.6. Petrogenetic model

The model including magmatic underplating and crustal anatexis in extensional tectonic environment was first applied to Finnish rapakivi granites by Haapala (1985, 1989) and Nurmi and Haapala (1986), and has been further developed in several papers (Rämö, 1991; Haapala and Rämö, 1992; Elo and Korja, 1993; Rämö and Haapala, 1996). A simplified two-stage model, based on the model of Huppert and Sparks (1988), is presented in Fig. 4b. The mafic rocks are derivatives of mantle magmas that evolved through variable crustal assimilation, local hybridization, and fractional crystallization. The felsic rocks are essentially crust derived, but probably have a mantle component, and evolved through minor assimilation, hybridization, and fractional crystallization. The erupted lavas formed volcanoes and lava and tuff plateaus above the plutonic rapakivi complexes, and were subsequently eroded away. This simple model explains the origin of the rapakivi granite magmas, bimodal character of the magmatism, thinning of the lower crust, and extensional setting, but does not explain the reason for the partial melting of the mantle. In this regard, possible mechanisms include passive or active rifting, deep mantle plumes, extensional collapse of the Paleoproterozoic orogen, mantle superswells under a Paleoproterozoic supercontinent, and melting of subcontinental mantle owing to instabilities related to distant subduction zones on the flanks of accretionally growing continents (see Rämö and Haapala, 1995; Haapala and Rämö, 1999; Åhäll et al., 2000).

In his discussion on the origin of Laurentia's Mesoproterozoic anorogenic granitic magmatism, Hoffman (1989) suggested that the mid-Proterozoic supercontinent thermally insulated the mantle beneath its interior causing convective large-scale upwelling—thousands of kilometers in diameter—of the heated mantle, which led to anorogenic magmatism across Laurentia. According to Hoffman (1989), inward mantle flow at the periphery of the growing supercontinent may contribute to the development of mantle upwelling beneath the interior of the supercontinent, to balance the downward mantle flow at the periphery. This model can be applied to the Fennoscandian rapakivi magmatism as well as, at 1.6 Ga, Fennoscandia was probably part of a supercontinent that included Laurentia and Amazonia (Pesonen and Mertanen, 2002). The thick continental crust provided a radiogenic thermal blanket below which the subcontinental mantle became heated, started to upwell and melt locally, eventually bulging up into the lower crust in areas where the heat flow was especially high or the crust weak (e.g., along deep fracture zones). The substantial thinning of the lower crust above subcircular mantle domes (e.g., the Wiborg batholith area; Figs. 1 and 4a, b) suggests that, in such cases, thinning was mainly caused by upwelling mantle magmas (magmatic underplating) and extensive melting of the lower crust. The latter was promoted by the fertile (juvenile) character of the newly formed Paleoproterozoic crust (cf. Anderson and Bender, 1989). Mantle upwelling and related reorganization of the crust stabilized lithosphere in one area, and mantle diapirism shifted to other areas, producing the area-constrained age groups (Fig. 1a). Possible subduction-related downward mantle flows at the margin of the accretionally growing continent at 1.65–1.5 Ga (see Åhäll et al., 2000) may have contributed to the onset of the mantle upwellings beneath the interior of the continent (cf. Hoffman, 1989).

## 3. The 1.7 Ga Shachang rapakivi pluton

### 3.1. Geologic setting

Several rift-related 1.70–1.68 Ga rapakivi granite plutons and related mafic rocks intruded Archean gneisses and migmatites in the northern part of the

North China (or Sino-Korean) craton. This Archean craton records continental growth from 3.85–3.55 to ~2.5 Ga (Liu et al., 1990; Wang et al., 1990). During the Paleoproterozoic, the craton was reworked by several tectonic events and became surrounded by orogenic belts in the south and east. Between 1.85 and 1.60 Ga, an E-trending 50- to 100-km-wide intracratonic rift developed and was the site of extensive continental sedimentation and igneous activity, including rapakivi granite.

The emplacement of the rapakivi granites and associated quartz syenites and mafic rocks (anorthosites, gabbros, diabase dikes) was controlled by three fault zones within the rift (Yu et al., 1994, 1996a; Fig. 5a). The U–Pb zircon ages of the rapakivi granites and quartz syenites show little variation: the Lanying

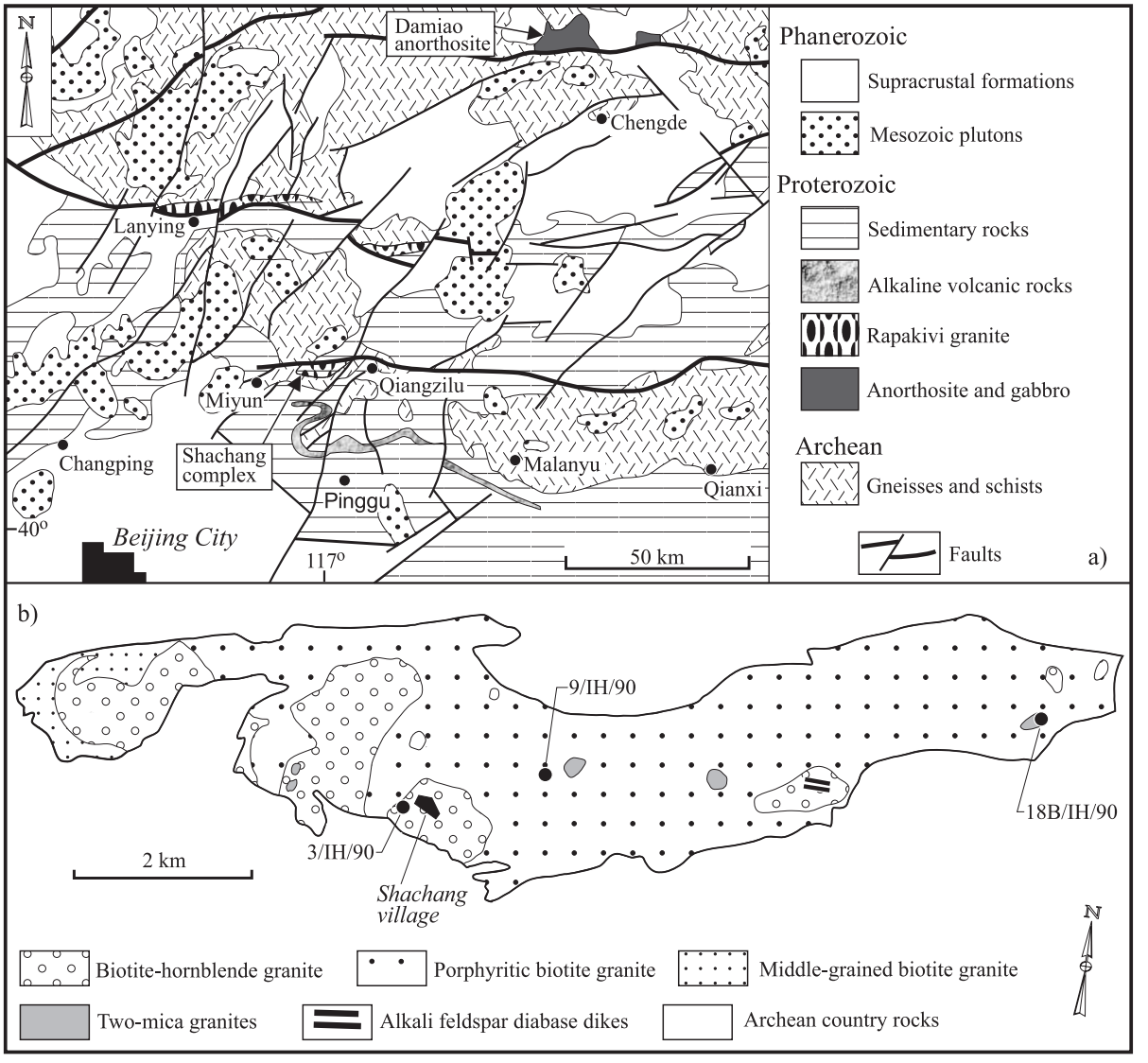



Fig. 5. (a) Geological map northeast of Beijing City showing the location of Proterozoic rapakivi granite–anorthosite–syenite complexes in relation to roughly E-trending fault zones. (b) The Shachang rapakivi granite pluton. The locations of representative type specimens (Table 1) are marked. Modified from Rämö et al. (1995).

pluton is 1697.3±4 Ma, the Chiecheng pluton (located west of the area shown in Fig. 4a) 1696.7±2.4 Ma, and the Shachang pluton 1690.5±2.4 to 1683.8±2.2 Ma (Yu et al., 1996a,b). The age of the Damio anorthosite–quartz mangerite complex is less accurate with an Sm–Nd isochron age of 1735±239 Ma for anorthosite and an Rb–Sr isochron age of 1686±193 Ma for quartz mangerite (Yu et al., 1996a).

During the Mesozoic, the Archean crust was intruded by granitic plutons, and the crust was ruptured along NE-trending faults. In spite of this, deep seismic sounding studies suggest an E-trending mantle dome under the Proterozoic rift where the rapakivi granites are found. In the area of Shachang complex, the crust is ~37 km thick (Yu et al., 1996a).

### 3.2. Petrography

The Shachang rapakivi granite pluton is located in the southern rift fault zone, 75 km northeast of Beijing City (Fig. 5). The complex is 13 km long and 0.5 to 2.5 km wide and cuts sharply the late Archean gneisses and migmatites. The pluton is composed of three granites. The earliest one is a rapakivi-textured

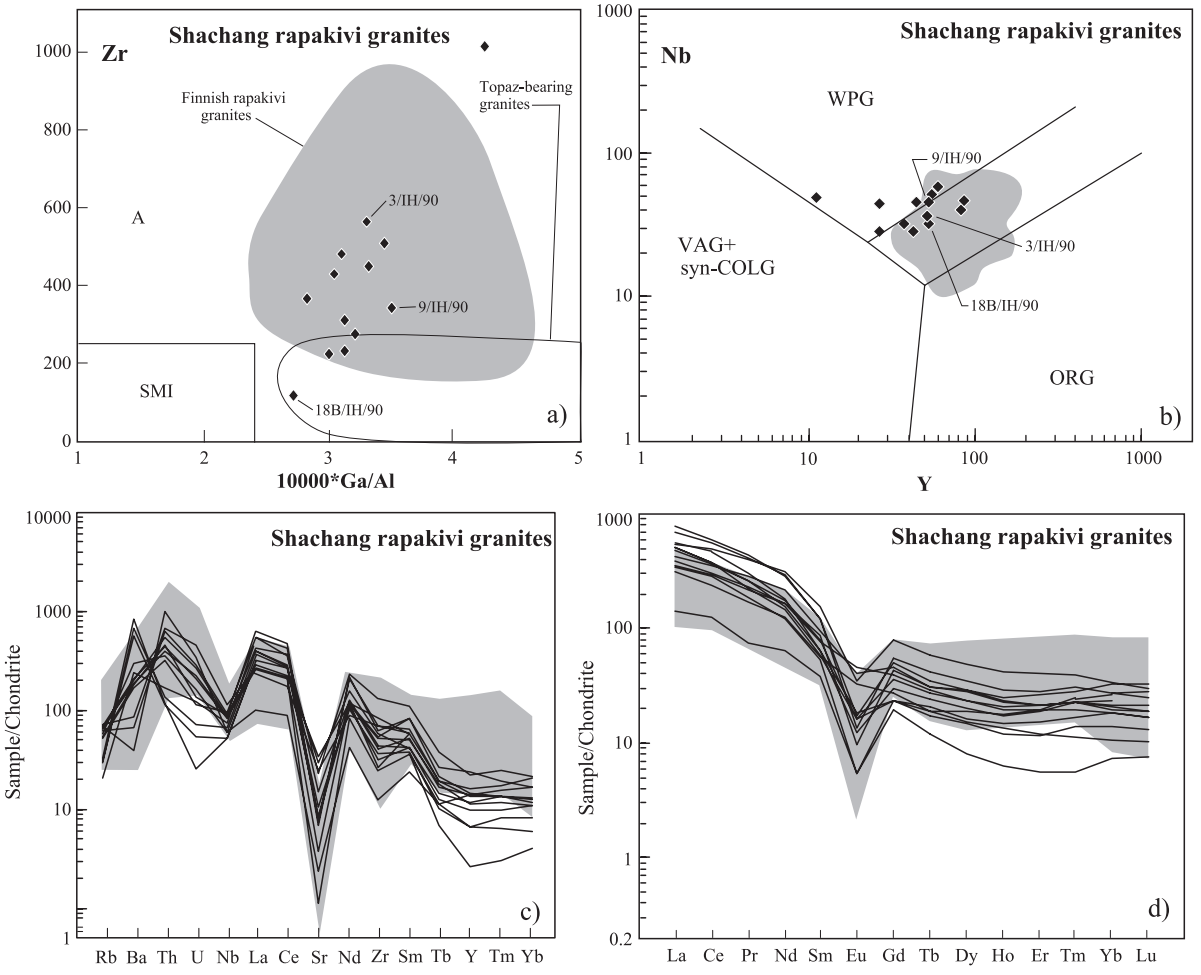



Fig. 6. Analyses of the Shachang rapakivi granite pluton (Rämö et al., 1995; Yu et al., 1996a,b) plotted in (a) Zr versus 10,000 Ga/Al (Whalen et al., 1987), (b) Nb versus Y (Pearce et al., 1984); (c) chondrite-normalized multielement, and (d) chondrite-normalized REE diagrams. The representative type samples (Table 1) are indicated in (a) and (b). The fields of the Finnish rapakivi granites (Fig. 3, shadowed) are indicated.

hornblende–biotite granite with rounded alkali feldspar megacrysts (6–8 cm in diameter) consisting of several sectorially intergrown crystal units; about one third of the ovoids have plagioclase shells. The mafic minerals are enriched in iron: Fe/(Fe+Mg) is 0.80–0.82 in hornblende and 0.76–0.92 in biotite. The prevailing granite type is a porphyritic biotite granite, and the westernmost part of the complex consists of a medium-grained biotite granite. The youngest intrusive phase is a medium- to fine-grained two-mica granite that occasionally also contains topaz. Wolframite-bearing quartz veins are found along the southern margin of the complex, and have been mined in the past.

Associated with the Shachang granites are felsic porphyry and diabase dikes. Two diabase dikes that cut the porphyritic hornblende–biotite granite contain abundant corroded alkali feldspar xenocrysts. These must have been derived from partially crystallized granitic magma and thus demonstrate the bimodal character of the magmatism.

### 3.3. Geochemistry and isotopes

In terms of their whole-rock and mineral chemistry, the Shachang granites resemble the rapakivi granites of Finland. They are metaluminous to peraluminous and plot in the discrimination diagrams in the fields of A-type and within-plate granites, thus overlapping with the Finnish rapakivi granites (Fig. 6a,b). In multielement and REE diagrams, the Shachang granites are nearly identical to the Finnish rapakivis (Fig. 6c,d).

Nd isotope data on 10 granite and 3 country rock samples are presented, together with data of the Finnish rapakivi granites, in Fig. 7 (cf. Rämö et al., 1995). The Shachang granites show uniform $\varepsilon_{Nd}$ (at 1685 Ma) values that average at $-5.7\pm0.3$ ($1\sigma$), and depleted mantle model ages ($T_{DM}$) of 2220 to 2410 Ma. The country rocks show $\varepsilon_{Nd}$ (at 2500 Ma) values of +0.6 to +1.5, and $T_{DM}$ ages of 2560 to 2630 Ma (Rämö et al., 1995). The data suggest that the late Archean crust was the main source of the Shachang

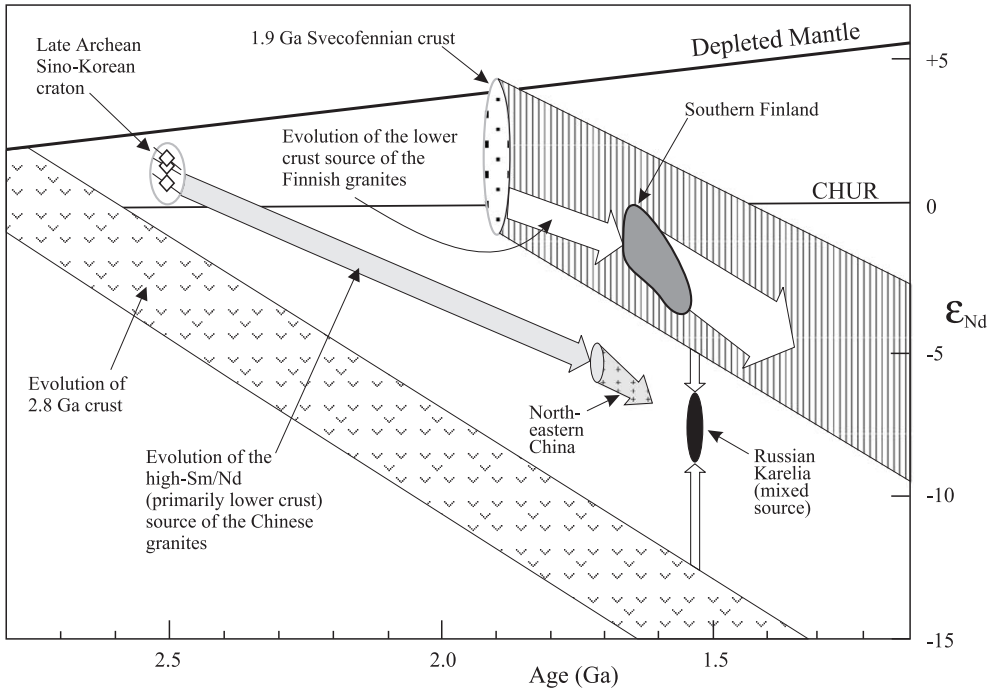



Fig. 7. $\varepsilon_{Nd}$ versus age diagram showing the initial Nd isotope composition of granites and the Archean country rocks of the Shachang rapakivi granite pluton (Rämö et al., 1995) as well as the rapakivi granites (Rämö, 1991) and the earlier Svecofennian igneous rocks (Huhma, 1986; Patchett and Kouvo, 1986) of Finland. The diagram also shows the evolution of the rapakivi granites and their probable sources in the Shachang area and in Finland, evolution of the undifferentiated Earth (CHUR; DePaolo and Wasserburg, 1976) and depleted mantle (DM; DePaolo, 1981).

rapakivi granites, possibly with minor mantle magma input. The granites are thus at least 800 Ma younger than their principal source. Compared to the Finnish rapakivis, the striking similarities regarding the magmatic association and chemical composition further suggest similar genetic processes (magmatic underplate) and approximately similar source regions.

## 4. The Cretaceous Gross Spitzkoppe granite, northwestern Namibia

### 4.1. Geologic setting

The Gross Spitzkoppe granite stock is one of about 20 anorogenic Mesozoic Damaraland plutonic complexes in the Pan-African (Neoproterozoic–Paleozoic) Damara orogenic belt of Namibia (Fig. 8). The Damara orogen can be divided into three branches: the northern (Kaoko belt) and southern (Gariep belt) branches that follow the Atlantic coast, and the NE-trending 400-km-wide inland branch (Damara belt). These mobile belts developed by amalgamation of three Precambrian cratons: the Congo craton in the north, the Kalahari craton in the south, and the Rio de la Plata craton in the west (Miller, 1983; Prave, 1996; Seth et al., 1998). The Damara orogenic belt was intensively metamorphosed and intruded by syn-orogenic to post-orogenic granitic-dioritic plutons at ~650–450 Ma (Miller, 1983).

The anorogenic Damaraland complexes include subvolcanic-epizonal complexes of three categories

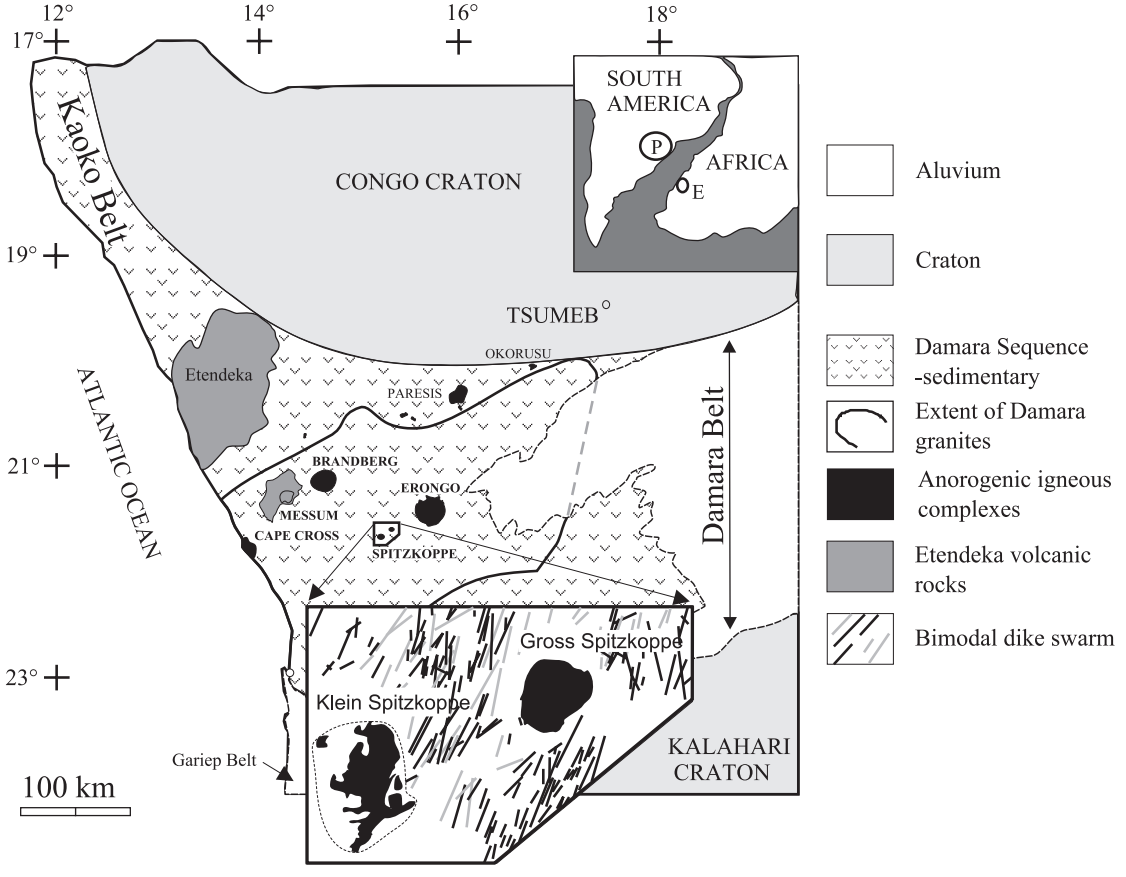



Fig. 8. Geological sketch map of northwestern Namibia showing the distribution of the Cretaceous 137–123 Ma Etendeka volcanic rocks and Damaraland volcanic-plutonic complexes. The lower inset shows the Gross Spitzkoppe and Klein Spitzkoppe granite stocks and bimodal dike swarms. In the upper inset map, P marks the bimodal Parana volcanic rocks in Brazil and E the corresponding Etendeka volcanic rocks in Namibia. Simplified from Miller (1983) and Milner et al. (1995).

(Martin et al., 1960; Milner et al., 1995): (1) granitic complexes (Brandberg, Erongo, Gross and Kleine Spitzkoppe); (2) differentiated basic complexes (e.g., Cape Cross, Messum, Okenjeje); and (3) peralkaline and carbonatitic complexes (e.g., Paresis, Kalkfeld, Okorusu). They extend in the Damara belt from the Cape Cross complex on the coast to the Okoruso complex about 350 km inland. Their isotopic Rb–Sr and Ar–Ar ages range from 124 to 137 Ma (Milner et al., 1995). Thus they are ~50–60 Ma younger than the Karoo basalts and more than 300 Ma younger than the post-orogenic (500–450 Ma) Damara granites. Associated with the Damaraland complexes are large amounts of diabase and quartz latite–rhyolite dikes and lavas (Fig. 8). The bimodal Etendeka lava field represents the eastern part of the wide 135–132 Ma Etendeka–Parana volcanic province.

The origin and emplacement of the Damaraland complexes and associated volcanic rocks and their counterparts along the Atlantic margin in South America has been related to the Tristan mantle plume, as well as to continental rifting that led to the opening of the southern Atlantic (O'Conner and le Roex, 1992; Milner and le Roex, 1996). The intracratonic rifting developed to seafloor spreading at 130 Ma, as can be judged from the oldest magnetic anomaly (M4) off the coast of Namibia (Rabinowitz and LaBrecque, 1979). Although the Damaraland–Parana lavas and intrusive complexes are found over a wide area, they were formed within a relatively short time period of ~15 Ma. The emplacement of the Damaraland intrusive complexes was controlled by old zones of weakness within the Damara orogenic belt between the Precambrian cratons (e.g., Milner et al., 1995). As in the Fennoscandian shield, the metasedimentary-metavolcanic mobile belt with old zones of weakness was more prone to heat flow and mantle diapirism than the Archean cratons.

Deep seismic reflection soundings suggest that, at the southern margin of the Damara belt, the crust is layered and more than 50 km thick. It is much thinner than this (with strongly reduced lower crust) in the central parts of the belt where the Damara and Damaraland granitic plutons are found (Green, 1983). This may be related to voluminous partial melting of the lower crust and extraction of granitic melts during the Damara orogen and Damaraland anorogenic event (Green, 1983; Ewart et al., 1998b).

### 4.2. Petrography

The Gross Spitzkoppe stock is an inselberg of an epizonal, rounded 30 km$^2$ granite complex that

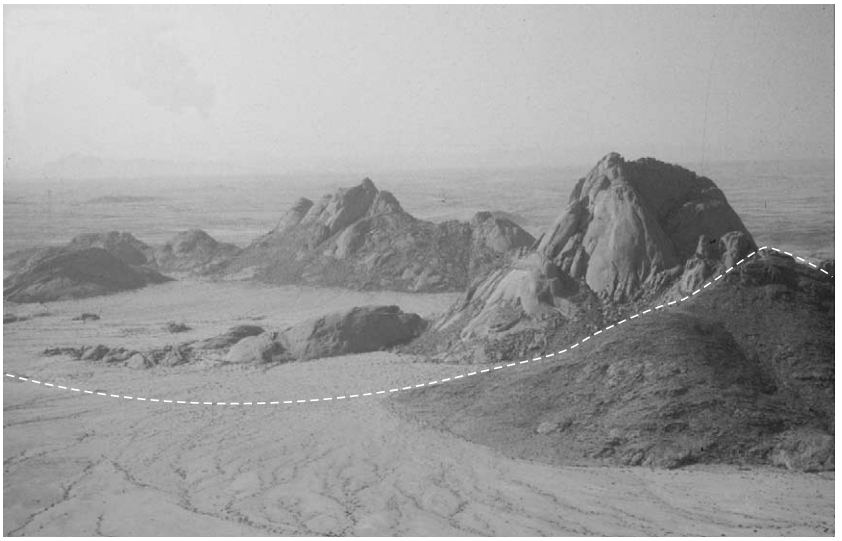


Fig. 9. An areal view from the northwest showing Gross Spitzkoppe (right) and Pondok (centre) mountains of the Gross Spitzkoppe stock. The outer limit of Gross Spitzkoppe stock in foreground is indicated by dashed line. Photo: Ilmari Haapala.

intrudes the Damara metasediments and granites (Figs. 9 and 10). The Damara crust is also cut by mainly NE- and NW-trending diabase and quartz latite dikes, which obviously represent the same magmatic event as the bimodal Etendeka volcanic rocks and are slightly older than the Gross Spitzkoppe and Klein Spitzkoppe granites. Bimodal character of the Spitzkoppe granite magmatism is indicated by synplutonic mafic dikes and magmatic mafic-intermediate inclusions, which contain quartz and alkali feldspar xenocrysts (Fig. 2e; Frindt, 2002; Frindt et al., 2004a). Locally, lamprophyric dikes cut the Spitzkoppe granites.

The Gross Spitzkoppe stock is composed of three zonally arranged granite types: medium-grained biotite granite at the margins, and a coarse-grained biotite granite and porphyritic biotite granite at the center. The outward dipping contact of the pluton as well as some inner contacts are marked by layered pegmatites and aplites, which show textures indicating crystallization from undercooled magma (Frindt and Haapala, 2002, 2004). The granites are cut by subhorizontal aplite dikes up to 20 m in width and by a number of variously dipping thinner pegmatite and aplite dikes. Miarolitic cavities and pegmatite pockets with topaz and beryl are common, indicating local fluid saturation. The porphyritic granite is occasionally greisenized and mineralized with wolframite; otherwise the granites are well preserved (Frindt and Poutiainen, 2002). The three granites are all topaz-bearing monzogranites that contain a few percent of extremely iron-rich biotite [(Fe/(Fe+Mg) 0.90 to 1.00]. Common accessory minerals include fluorite, columbite, monazite, zircon, magnetite, and niobian rutile.

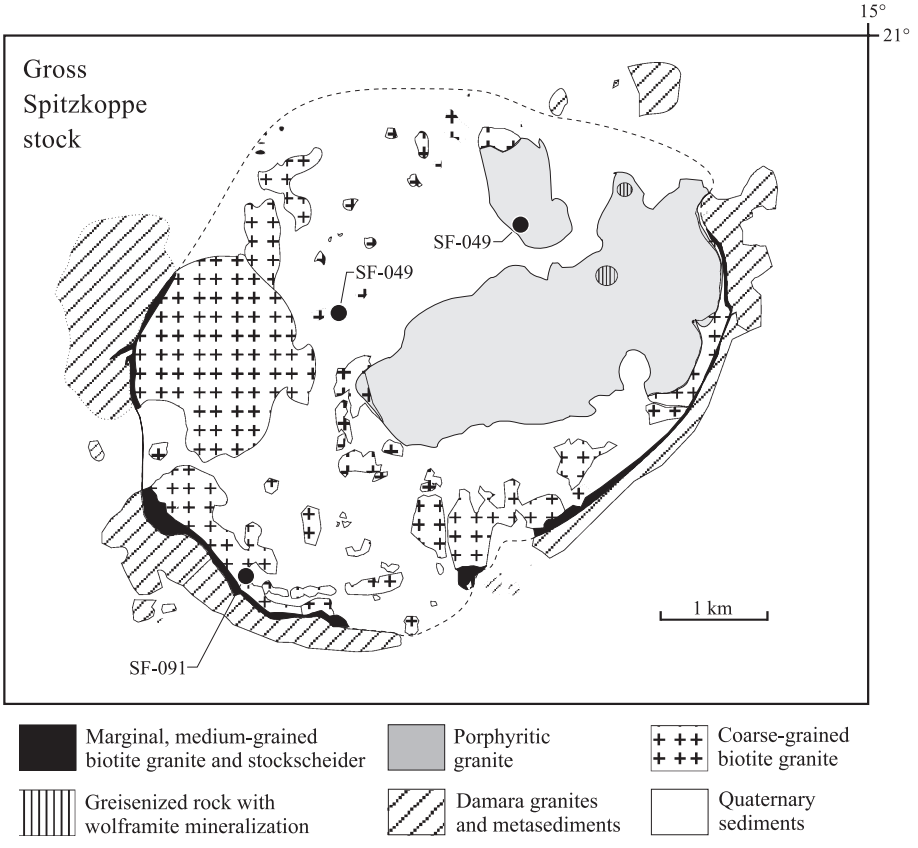



Fig. 10. Geological map of the Gross Spitzkoppe granite stock. The locations of representative type specimens (Table 1) are marked. Adopted from Frindt and Haapala (2002) and Frindt (2002).

### 4.3. Geochemistry, isotopes, and petrogenesis

The granites are marginally peraluminous high-silica monzogranites and, in all discrimination diagrams, plot into the fields of A-type and within plate granites, just like the rapakivi granites of Finland (Fig. 11). There are only minor differences in the average composition of the different granite types (Frindt et al., 2004a): $SiO_2$ 75.7–76.6, $Al_2O_3$ 12.22–12.48, $Fe_2O_3$ 1.45–1.71, FeO 0.80–1.07, MgO 0–0.01, CaO 0.37–0.76, $Na_2O$ 3.19–3.46, $K_2O$ 5.04–5.53, and F 0.47–0.51 wt.%. $Na_2O+K_2O$ is high, on average 8.45 wt.%. The granites belong to the "low-P" subtype ($P_2O_5$<0.1, $Al_2O_3$<14.5, $SiO_2$>73 wt.%) of F-rich granites by Taylor (1992). In the normative Ab–Or–Q diagram, they plot near the ternary minimum with 0.5 wt.% F at 1 kbar water pressure. High contents of incompatible trace elements (Rb ranges from 446 to 831, Nb from 60 to 176, Ta from 3.0 to 15, and Ga from 24 to 42 ppm) as well as low contents of Sr (5 to 48 ppm), Ba (0 to 164 ppm), and Eu/Eu* (0.23 to 0.00) suggest a high degree of fractionation (Frindt et al., 2004a). The granites show many geochemical similarities with the topaz-bearing rapakivi granites of Finland (Fig. 11a–d) but also some differences. The Sn contents are elevated (11 to 14 ppm), but not so high as in typical tin granites. The sum of alkalies is higher than in the Finnish rapakivi granites with corresponding silica contents. Accessory magnetite is ubiquitous in the Spitzkoppe granite but ilmenite is very rare. This indicates more oxidizing conditions in the Spitzkoppe granites than in the Finnish rapakivis.

Isotopic studies (Rb–Sr, Ar–Ar, Sm–Nd, Rb–Sr) have recently been published from the Etendeka and

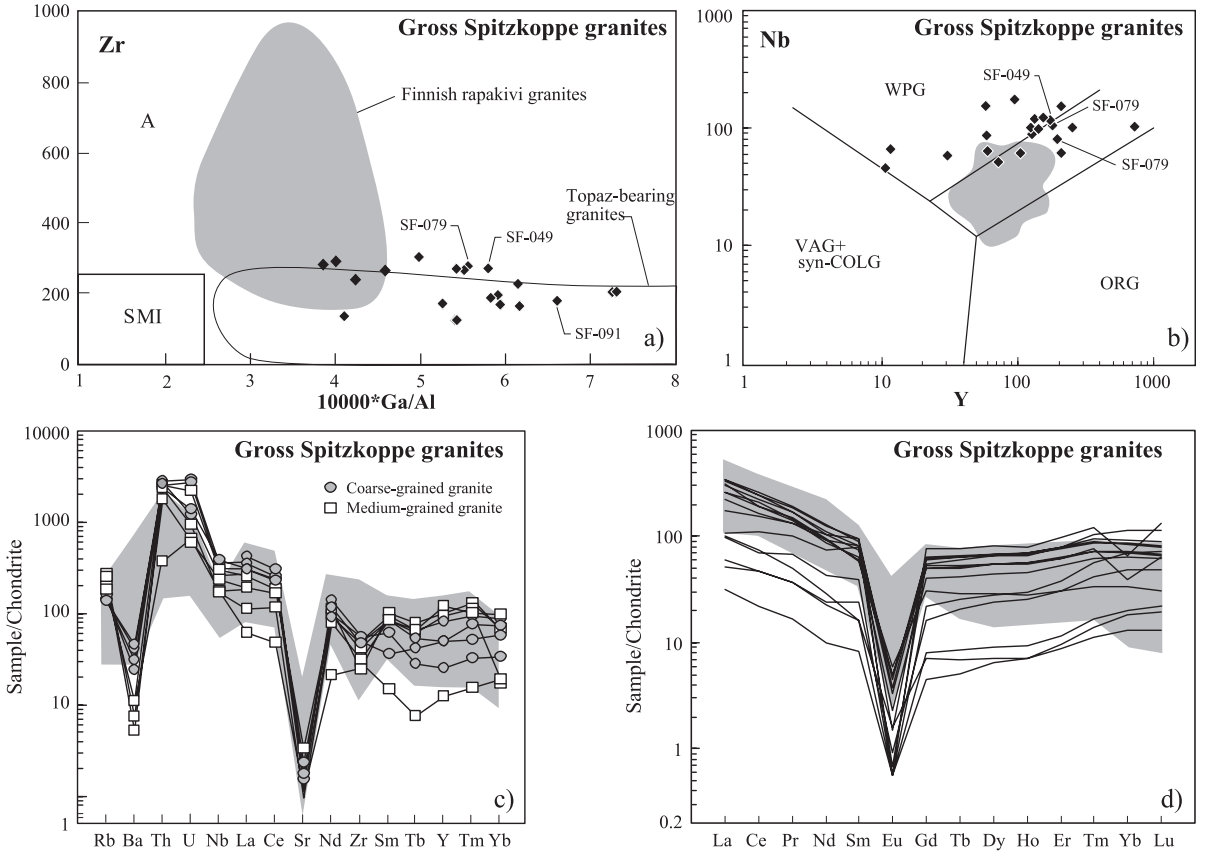



Fig. 11. Analyses of the Gross Spitzkoppe granites plotted in (a) Zr versus 10,000 Ga/Al (Whalen et al., 1987), (b) Nb versus Y (Pearce et al., 1984), (c) chondrite-normalized multielement, and (d) chondrite-normalized REE diagrams. The representative type samples (Table 1) are indicated in (a) and (b). The fields of the Finnish rapakivi granites (Fig. 3, shadowed) are shown.

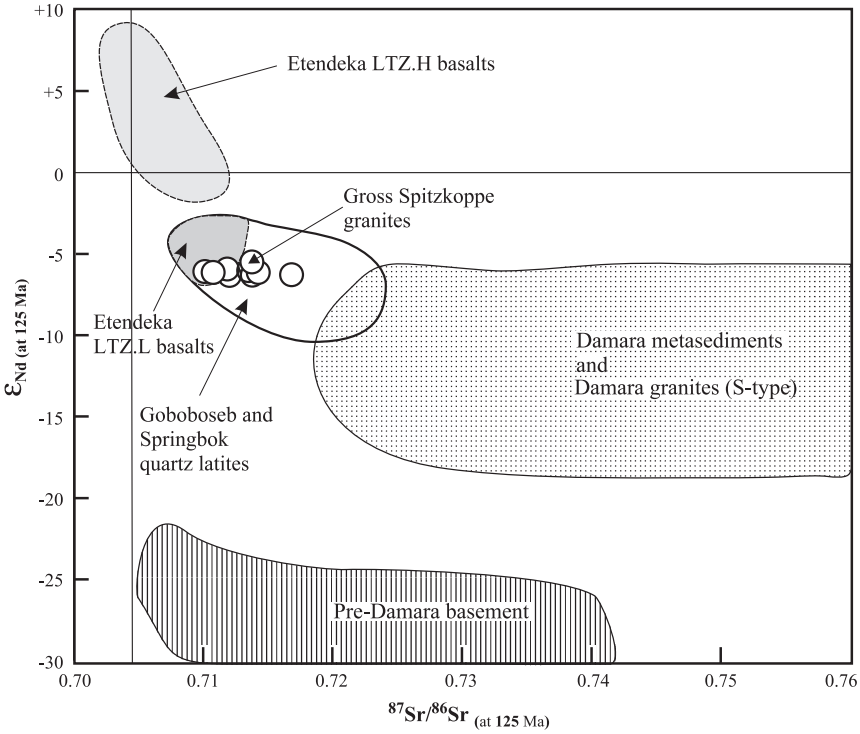



Fig. 12. Initial Nd–Sr isotope compositions (calculated at 125 Ma) of the Gross Spitzkoppe granites (open circles; Frindt, 2002), compared to the fields of pre-Damara basement (Seth et al., 1998), Damara metasediments and S-type granites (McDermott and Hawkesworth, 1990; McDermott et al., 1996), Etendeka LTZ.H and LTZ.L basalts and Goboboseb and Springbok quartz latites (Ewart et al., 1998a,b).

Messum lavas (Milner et al., 1995; Ewart et al., 1998a,b) and from the Brandberg granite complex (Schmitt et al., 2000). These indicate that, in northwestern Namibia, there are two major types of tholeiitic basalts. LTZ.H basalts (low Ti and Zr; high Ti/Zr) with $\varepsilon_{Nd}$ (at 132 Ma) values of +6.2 to +1.0 and initial $^{87}Sr/^{86}Sr$ ratios, $Sr_i$, of 0.704 to 0.705 represent dominantly mantle plume melts, whereas LTZ.L basalts (low Ti and Zr; low Ti/Zr) with $\varepsilon_{Nd}$ (at 132 Ma) values of −8.0 to −9.5 and $Sr_i$ of 0.708–0.717 represent plume–crust interactions and fractionation (Ewart et al., 1998a). The associated quartz latites with $\varepsilon_{Nd}$ (at 132 Ma) values of −7.3 to −9.0 and $Sr_i$ of 0.7175 to 0.7211 are hybrids involving high degrees of lower and upper crustal melting and fractionation. The metaluminous and peralkaline granites of the Brandberg complex have $\varepsilon_{Nd}$ (at 130 Ma) values of −0.4 to −5.1 and $Sr_i$ of 0.707 to 0.727, suggesting a major crustal source component (Schmitt et al., 2000) and significant mantle input. Preliminary isotope studies by Trumbull et al. (2000) and Frindt et al. (2004b) on the Gross Spitzkoppe granitic stock show a dominant (60–75%) crustal isotopic signature (Fig. 12), and a significant (25–40%) mantle component. Geochemical constraints suggest that the parent magmas of the quartz latite dikes (and possibly also the Gross Spitzkoppe granites) were formed by partial (10–20%) melting of felsic granulite (Frindt et al., 2004b).

## 5. Miocene basalt–rhyolite–granite association, southern Nevada

### *5.1. Geologic outline of the Basin and Range Province*

The geologic history of the Basin and Range Province (BRP) of the southwestern United States extends from the Precambrian to today. The basement is composed mainly of Paleoproterozoic (~1.7 Ga) high- to medium-grade gneisses, which were intruded by mid-Proterozoic ~1.4 Ga granites. In the northern

part of the BRP, the basement consists of the Archean rocks of the Wyoming Province. During late Paleozoic, the coast of southwest America became an active continental margin. Eastward subduction continued through the Mesozoic leading to a succession of orogenic events and igneous activity and accretionary growth of the continent. The Cretaceous magmatic arc is represented by the 135 to 80 Ma granitic batholiths of Baja California, Sierra Nevada, and Idaho. From the mid-Cretaceous to early Paleogene, the rocks of the continental margin were thrust eastward, giving rise to a foreland fold-and-thrust belt (Hamilton, 1987). The rapid eastward accretion and thrusting during the late Cretaceous–Paleogene Sevier-Laramide orogenies led to major crustal shortening and thickening of the orogenic crust.

The rapid subduction related to the Sevier-Laramide orogenies led to the arrival of the East Pacific spreading axis at the trench at about 30 Ma. Consumption of the Farallon plate was accompanied by steepening and cessation of the subduction, development of the San Andreas transform fault zone, and strong extension (BRP; Coney, 1987; Wernicke, 1985; Hodges and Walker, 1992). Active extension and rifting was accompanied by magmatism, which changed gradually and with some overlapping from intermediate-felsic calc-alkaline to bimodal basaltic-rhyolitic A-type magmatism. Although active debate continues about the details, the general interpretation is that this change in composition of the Tertiary magmatism reflects the change from plate subduction magmatism to continental rift magmatism.

The Tertiary extension was quite pronounced in the 50- to 100-km-wide NW-trending zone known as the Colorado River extensional corridor (CREC; Fig 13). This zone is characterized by extensive normal and listric faulting, large-scale subhorizontal detachment faults, and a central zone of tectonically uplifted domal metamorphic core complexes (Howard and John, 1987; McCarthy et al., 1991; Howard et al., 1994). Bimodal volcanism overlapped with extension, and several granitic plutons of this age are now exposed—one of them is the Spirit Mountain pluton (SMP). Strong extension led to thinning of the crust from about 60 to 26–30 km (McCarthy et al., 1991; Zandt et al., 1995). This thinning was especially strong in the lower crust. Although the extension and magmatism overlapped in time, there are indications that in some cases the magmatism started first and extension followed thereafter (e.g., Gans et al., 1989; Scott et al., 1995). Debate continues on whether the extension (decompression) was the cause or effect of mantle magmatism.

The Miocene bimodal extension-related magmatism in BRP is mainly represented by basaltic and rhyolitic volcanites and dikes, but in places also high-level plutonic members, including rapakivi-textured granites, are known (Volborth, 1973; Calzia, 1994; Calzia and Rämö, 2000). Some of the rhyolites are topaz-bearing and may host Sn–Be–W mineralization (Christiansen et al., 1986; Congdon and Nash, 1991).

### 5.2. Petrography

The Newberry Mountains in the CREC host three Tertiary granite plutons surrounded by Proterozoic granites and gneisses (Fig. 13): the White Rock Wash pluton (WRWP), the Spirit Mountain pluton (SMP), and the Mirage pluton (MP) (Volborth, 1973; Howard et al., 1994; Haapala et al., 1995; Rämö et al., 1999).

WRWP consists of a medium- to coarse-grained two-mica granite, which shows deformation and recrystallization, and gives an ion probe U–Pb age of 68.5 Ma (Miller et al., 1997) and a whole-rock Rb–Sr age of about 65 Ma (Rämö et al., 1999). Petrographically, it is similar to the Cretaceous two-mica granites in the Eldorado Mountains (D'Andrea Kapp et al., 2002) and elsewhere in the Cordillerian interior (Miller and Barton, 1990). Plagioclase is more abundant than alkali feldspar. Magnetite, apatite, and zircon are common accessory minerals, and garnet is locally present. In places, the granite shows gradual migmatitic contacts with surrounding Proterozoic mica gneisses. Its origin and emplacement is related to thrusting and crustal thickening at the convergent plate boundaries during late stages of the Sevier orogeny.

SMP is mainly composed of a medium- to coarse-grained weakly porphyritic biotite±hornblende granite (Spirit Mountain granite) and gives a whole-rock Rb–Sr age of ~20 Ma (Rämö et al., 1999). Part of the alkali feldspar megacrysts are mantled by plagioclase. Magnetite and titanite are characteristic minor constituents and apatite, zircon, and allanite are present in small amounts. At the western margin of the pluton, the Spirit Mountain granite grades into a fine- to

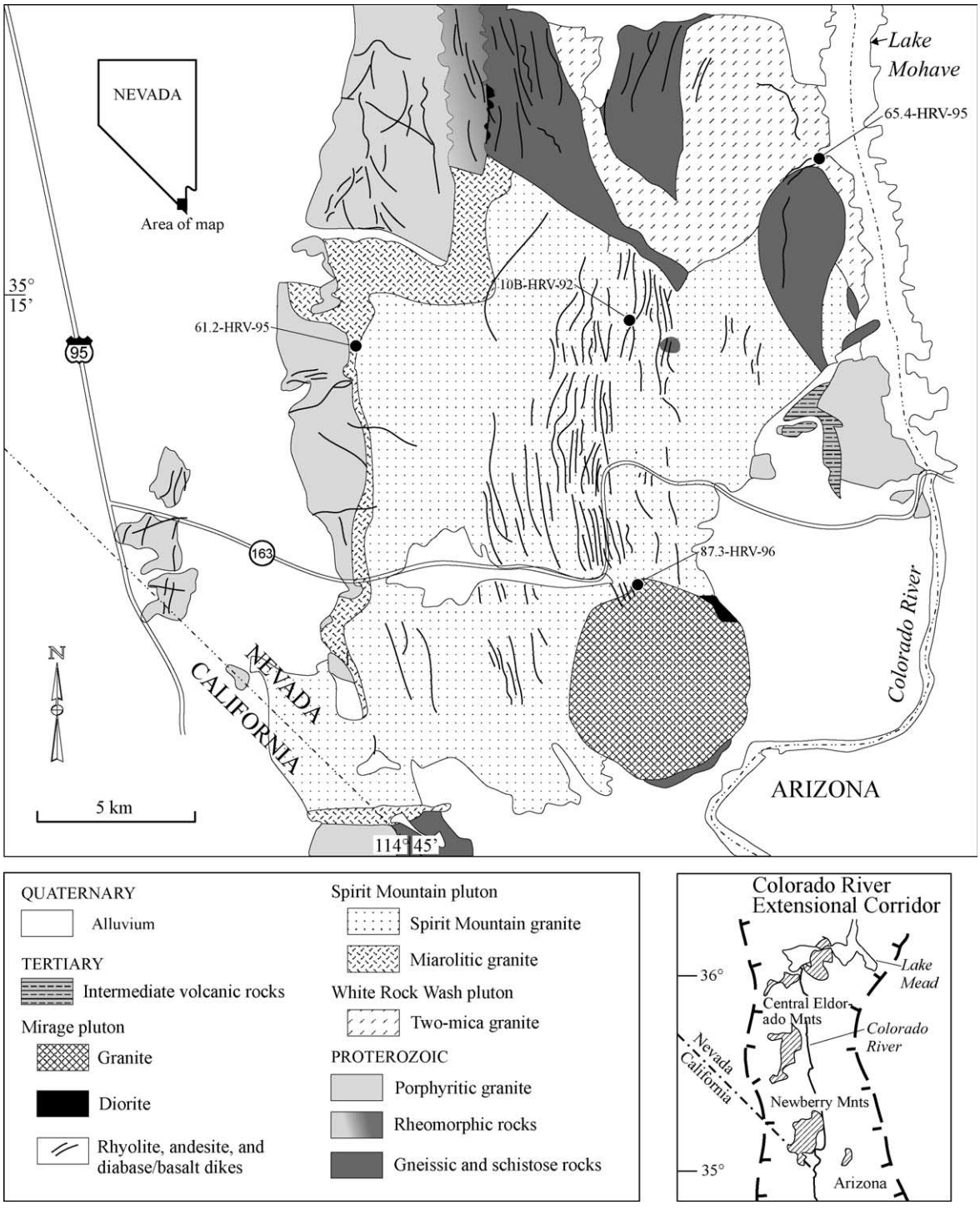



Fig. 13. Geological map of the Newberry Mountains area in southern Nevada, based on Volborth (1973) and 1992–1996 field studies by I. Haapala, O.T. Rämö, and A. Volborth. The locations of representative type specimens (Table 1) are marked. The inset shows location of the study area (Newberry Mountains) relative to the Colorado River extensional corridor.

medium-grained, granophyric and miarolitic alkali feldspar granite (Volborth, 1973). Perthitic alkali feldspar is the prevailing or sole feldspar and muscovite and biotite are locally present. Minor fluorite is also commonly present. The miarolitic granite probably represents the apical parts of the magma chamber and suggests westward tilting of the pluton during rifting.

MP consists of fine- to medium-grained biotite granite, which usually is porphyritic but may grade into an even-grained microgranite; dioritic rocks are found in the northeastern and southeastern margin of the pluton. The texture is hypidiomorphic with euhedral andesine and biotite crystals, biotite is often chloritized. Magnetite, apatite, and zircon are typical accessory minerals. According to Howard et al. (1994), all the Miocene dike swarms and plutons in the southern Newberry Mountains are probably 18–14 Ma in age.

The Tertiary granite plutons and their Precambrian country rocks are cut by numerous, generally NS-striking mafic and rhyolite dikes. Some dikes yield spectacular examples of mingling and hybridization of the two magmas (Volborth, 1973).

### 5.3. Geochemistry

The three granite plutons are distinct from each other in chemical composition (Table 1; Fig. 14a–f). The WRWP granites are peraluminous with molecular $Al_2O_3/(CaO+Na_2O+K_2O)$ (A/CNK) varying from 1.0 to 1.15, whereas the granites of SMP and MP straddle the metaluminous-peraluminous boundary (SMP 0.93–1.04, MP 0.98–1.08). In the Spirit Mountain granite, the one with mantled alkali feldspar megacrysts, $SiO_2$ varies from 66.6 to 76.4 wt.%, and $Na_2O+K_2O$ from 8.2 to 9.6 wt.%. SMP has the highest K/Ca and Rb/Ba, MP the highest Ca, Mg and Fe, and WRWP the highest Na/K and lowest Rb/Ba. The miarolitic granite of SMP is geochemically the most evolved with lowest Ti, Mg, Ba, and Sr, and highest Rb and F. SMP has a clear negative Eu/Eu* anomaly, which is deepest in the miarolitic granite (Fig. 14d,f).

In the discrimination diagrams of Whalen et al. (1987), the MP granite plots into the field of I, S, M-type granites, whereas the SMP and WWP plot in both A- and I, S, M-fields (Fig. 14a). In the diagrams of Pearce et al. (1984), the SMP granites plot into the within plate granite fields, and those of WWP and MP into the fields of volcanic arc granites (Fig. 14b). The multielement spidergram and REE diagram of the SMP granites show similarities with the rapakivi granites of Finland (Fig. 14c,d), whereas the corresponding diagrams of WRWP and MP differ markedly from them (Fig. 14e,f).

The granite plutons of the Newberry Mountains provide an example of the flaws involved in the use of tectonomagmatic discrimination diagrams. Although both SMP and MP appear to be synextensional and related to continental rifting, only the SMP granites plot into the within-plate granite field. Similar observations have been made by several authors (Falkner et al., 1995, and references therein). Extensional processes were intimately associated with magmatic underplating, which hybridized the lithosphere shortly after cessation of convergence (see Falkner et al., 1995; Rämö et al., 1999; Miller and Miller, 2002). In such rapidly changing tectonic regime, sources generated at pre-, syn-, and post-hybridization stages can yield typologically different granites.

### 5.4. Isotope studies and petrogenesis

Preliminary Nd, Pb, and Rb–Sr isotopic studies on the plutons and diabase dikes of the Newberry Mountain area have been presented by Haapala et al. (1995, 1996) and Rämö et al. (1999). The Nd isotopic results are summarized in Table 2 and Fig. 15.

The WRWP has $\varepsilon_{Nd}$ (at 65 Ma) values of $-16.2\pm0.3$ Ma and Nd model ages averaging $1766\pm100$ Ma (Rämö et al., 1999). This indicates a major Proterozoic source. SMP has $\varepsilon_{Nd}$ (at 20 Ma) values of $-10.1\pm0.8$ Ma and Nd model ages averaging $1222\pm74$ Ma, which indicates clearly younger overall source. MP has isotopic composition between SMP and WRWP: $\varepsilon_{Nd}$ (at 15 Ma) ranges from $-11.4$ to $-14.2$ and Nd model ages from 1338 to 1552 Ma. The corresponding Sr isotope initial values are for WRWP $0.7119\pm0.006$, for SMP $0.7098\pm0.0002$, and for MP 0.7109 to 0.7115 (Rämö et al., 1999). Three diabase dikes from SMP have $\varepsilon_{Nd}$ (at 15 Ma) values of 0, $-4.1$, and $-8.4$, suggesting variable crustal contamination or a variably enriched mantle source.

Table 1
Representative chemical composition of the granites studied: wiborgite batholith and topaz granite stocks (Finland); Shachang (China); Gross Spitzkoppe (Namibia); Newberry Mountains (southern Nevada): Spirit Mountain (SM) pluton, Mirage (M) pluton, White Rock Wash (WRW) pluton

| | Finnish rapakivi granites | | | | | Shachang rapakivi | | | Gross Spitzkoppe | | | Newberry Mountains | | | |
|---|---|---|---|---|---|---|---|---|---|---|---|---|---|---|---|
| | | | Topaz granites | | | | | | Topaz granites | | | SM pluton | | M pluton | WRW pluton |
| | Wiborgite | Pyterlite | Eurajoki | Kymi | Suomenniemi | Wiborgite | Porphyritic granite | Fine-grained two-mica granite | Medium-grained granite | Coarse-grained | Porphyritic granite | Main granite | Miarolitic granite | Main granite | Two-mica granite |
| Sample # | 1A/IH/2001 | 2A/IH/2001 | 5/IH/2001 | 1/IH/89 | SMN-A1097 | 3/IH/90 | 9/IH/90 | 18B/IH/90 | SF-091 | SF-049 | SF-079 | 10B-HRV-92 | 61.2-HRV-95 | 87.3-HRV-96 | 65.4-HRV-95 |
| $SiO_2^I$ (wt.%) | 69.96[2] | 76.70[2] | 75.78[2] | 73.5 | 74.1 | 68.00 | 72.90 | 74.80 | 76.9 | 74.90 | 76.20 | 73.20 | 76.50 | 70.00 | 73.30 |
| $TiO_2^I$ | 0.42[2] | 0.18[2] | 0.02[2] | 0.02 | 0.04 | 0.60 | 0.24 | 0.09 | 0.04 | 0.13 | 0.10 | 0.29 | 0.07 | 0.36 | 0.18 |
| $Al_2O_3^I$ | 13.41[2] | 11.70[2] | 13.62[2] | 15.1 | 14.4 | 14.20 | 12.90 | 13.00 | 12.6 | 12.40 | 11.90 | 14.00 | 12.20 | 14.80 | 15.20 |
| $FeO^W$ | 3.35 | 1.53 | 0.65 | 0.6 | 0.1 | 2.20 | 0.80 | 0.10 | 0.7 | 1.20 | 1.00 | 0.7 | 0.10 | 1.1 | 0.60 |
| $Fe_2O_3^I$ | 0.45[2] | 0.31[2] | 0.19[2] | 0.2 | 0.81 | 1.72 | 1.44 | 0.96 | 1.24 | 1.81 | 1.70 | 1.06 | 0.63 | 1.35 | 0.69 |
| $MnO^I$ | 0.06[2] | 0.02[2] | 0.05[2] | 0.02 | 0.02 | 0.00 | 0.04 | 0.02 | 0.01 | 0.02 | 0.01 | 0.05 | 0.07 | 0.04 | 0.02 |
| $MgO^I$ | 0.35[2] | 0.09[2] | 0.00[2] | 0.1 | 0.01 | 0.49 | 0.15 | 0.08 | 0.00 | 0.00 | 0.00 | 0.51 | 0.01 | 0.74 | 0.31 |
| $CaO^I$ | 2.16[2] | 0.80[2] | 0.64[2] | 0.76 | 0.99 | 1.85 | 1.11 | 0.79 | 0.36 | 0.82 | 0.77 | 1.08 | 0.47 | 2.21 | 1.85 |
| $Na_2O^I$ | 3.09[2] | 2.49[2] | 3.70[2] | 4.05 | 4.32 | 3.59 | 3.43 | 3.80 | 3.71 | 3.20 | 3.18 | 3.98 | 4.06 | 3.67 | 4.40 |
| $K_2O^I$ | 5.46[2] | 5.59[2] | 4.35[2] | 4.55 | 4.14 | 5.23 | 5.29 | 5.37 | 4.93 | 5.48 | 5.09 | 4.87 | 4.54 | 4.35 | 3.10 |
| $P_2O_5^I$ | 0.11[2] | 0.02[2] | 0.02[2] | 0.01 | 0.02 | 0.14 | 0.04 | 0.0 | 0.02 | 0.02 | 0.00 | 0.06 | 0.01 | 0.13 | 0.06 |
| $H_2O^{+\ W}$ | 0.31 | 0.17 | 0.24 | 0.4 | na | 0.90 | 0.50 | 0.4 | 0.2 | 0.30 | 0.20 | 0.4 | 0.20 | 0.50 | 0.30 |
| $F^W$ | 0.24 | 0.43 | 1.19 | 1.45 | 0.88 | 0.26 | 0.59 | 0.49 | 0.49 | 0.58 | 0.50 | 0.08 | 0.15 | 0.05 | 0.04 |
| Total | 99.37 | 100.03 | 100.43 | 100.76 | 99.83 | 99.18 | 99.43 | 99.91 | 101.20 | 100.86 | 100.65 | 100.28 | 99.01 | 99.30 | 100.05 |
| $-O=F_2$ | 0.10 | 0.18 | 0.50 | 0.61 | 0.37 | 0.11 | 0.25 | 0.21 | 0.21 | 0.24 | 0.21 | 0.03 | 0.06 | 0.02 | 0.02 |
| Total | 99.27 | 99.85 | 99.93 | 100.15 | 99.46 | 99.07 | 99.18 | 99.70 | 100.99 | 100.62 | 100.44 | 100.25 | 98.95 | 99.28 | 100.03 |
| $Cl^W$ (ppm) | 800 | 300 | 100 | 110 | na | 563[1] | 317[1] | 200[1] | 131 | 271 | 218 | na | na | na | na |
| $Rb^1$ | 271[4] | 349[4] | 1050[4] | 978 | 714 | 160 | 335 | 346 | 831 | 470 | 455 | 139 | 316 | 123 | 89 |
| $Sr^2$ | 155 | 69 | 8 | 22 | 16[1] | 558[1] | 171[1] | 53[1] | 15 | 23 | 19 | 159 | 12 | 338 | 527 |
| $Ba^1$ | 1144[2] | 541[2] | 28[2] | 151 | 118 | 2890 | 864 | 203 | 30 | 112 | 90 | 398 | 68 | 1240 | 965 |
| $Ga^4$ | 27 | 24 | 60 | 61[2] | 24 | 25[2] | 24[2] | 19[2] | 44[1] | 38[1] | 35[1] | 20 | 22 | 19 | 20 |
| $Be^2$ | 5 | 5 | 16 | 17 | na | 7 | 7 | 32 | 7 | 5 | 5 | 5 | <1 | 2 | <1 |
| $Zn^2$ | 125 | 86 | 197 | 67.2 | 28[1] | 87.6 | 39.5 | 21 | 55.6 | 44.9 | 40.9 | 6.7 | 7.4 | 5.6 | 39 |
| $Sc^2$ | 8[3] | 3[3] | 12[3] | 8 | 3.3[3] | 6.5 | 2.4 | 0.7 | na | na | na | 23 | 12 | 4 | 2 |
| $Zr^1$ | 459[4] | 304[4] | 51[4] | 12 | 39 | 560 | 340 | 116 | 179 | 271 | 280 | 184 | 119 | 135 | 119 |
| $Hf^3$ | 12.7 | 10 | 5.7 | 7.9 | 2.6 | 15 | 11 | 6.7 | 8.9 | 8.3 | 8.2 | 6.7 | 7.4 | 5.6 | 3.9 |
| $Sn^4$ | 8 | 9 | 110 | 15[1] | 35[1] | <2[1] | 27[1] | 28[1] | 18 | 14 | 12 | 23 | 12 | 2 | 15 |

| | | | | | | | | | | | | | | | |
|---|---|---|---|---|---|---|---|---|---|---|---|---|---|---|---|
| W[3] | 3 | 3 | 9 | 23 | na | 4 | 4 | 26 | 5 | 4 | 2 | 10 | 3 | na | 2 |
| Nb[1] | 26.4[4] | 25.8[4] | 69.8[4] | 58 | 50.7 | 37 | 46 | 33 | 82 | 120 | 107 | 39 | 51 | 14 | 10 |
| Ta[3] | 2.3[4] | 2.41[4] | 22.6[4] | 45 | na | 1 | 3 | 1.0 | 13 | 7.7 | 7.7 | 1.5 | 4 | <0.5 | 1.1 |
| Th[3] | 24.7[4] | 38.6[4] | 27.6[4] | 31 | na | 8 | 23 | 51.0 | 61 | 93 | 88 | 24 | 50 | 19 | 5.4 |
| U[3] | 8.08[4] | 14.7[4] | 6.34[4] | 35 | na | 1 | 3 | 5.4 | 7 | 27 | 28 | 2.3 | 4.6 | 1.5 | 1.5 |
| Pb[2] | 38 | 55 | 88 | 130 | na | 21 | 41 | 38 | 26 | 26 | 23 | 17 | 26 | 17 | 15 |
| Y[1] | 63[2] | 75[2] | 55[2] | 7[2] | 59 | 51[2] | 52[2] | 52[2] | 199 | 174 | 182 | 24 | 19 | 19 | 11 |
| La[4] | 95.9 | 99 | 47.4 | 65 | 28.1 | 155.0 | 176.0 | 52.7 | 39 | 131 | 125.0 | 51.6 | 27 | 44.5 | 26.3 |
| Ce[4] | 182 | 182 | 97.2 | 154 | 73.2 | 338.0 | 345.0 | 121.0 | 105 | 253 | 233.0 | 100 | 45 | 85.9 | 52.1 |
| Pr[4] | 21.5 | 21.2 | 11.1 | 15 | 8.6 | 39.4 | 35.8 | 10.2 | 13.9 | 26.7 | 25.5 | 9.9 | 3.4 | 9.1 | 5.7 |
| Nd[4] | 80.6 | 76.2 | 37.3 | 34.9 | 30.95 | 154.0 | 123.0 | 45.6 | 53.2 | 90.6 | 87.9 | 31.5 | 7.4 | 29.4 | 20.4 |
| Sm[4] | 14.6 | 13.7 | 9.26 | 8.1 | 8.55 | 22.2 | 18.2 | 8.7 | 18.6 | 20.8 | 21.9 | 5.8 | 1.4 | 5.3 | 3.7 |
| Eu[4] | 2.56 | 1.26 | 1.18 | <0.05 | 0.1 | 3.6 | 1.4 | 0.5 | 0.1 | 0.4 | 0.3 | 0.77 | 0.1 | 1.2 | 1.18 |
| Gd[4] | 12.6 | 12.2 | 7.77 | 3.2 | 7.4 | 14.0 | 10.9 | 7.1 | 16.6 | 19 | 19.5 | 4.8 | 1.5 | 4.5 | 3 |
| Tb[4] | 2.14 | 2.2 | 1.84 | 1.4 | 1.6 | 1.8 | 1.6 | 1.1 | 3.5 | 3.7 | 3.8 | 0.7 | 0.2 | 0.6 | 0.3 |
| Dy[4] | 12.7 | 13.8 | 12.7 | 9.7 | 13.6 | 10.7 | 8.8 | 7.2 | 24.9 | 25.8 | 25.6 | 4.1 | 1.9 | 3.3 | 2.1 |
| Ho[4] | 2.67 | 2.98 | 2.71 | 1.98 | 3.19 | 1.9 | 1.8 | 1.5 | 5.7 | 5.9 | 5.9 | 0.84 | 0.5 | 0.6 | 0.38 |
| Er[4] | 7.26 | 8.51 | 8.6 | 8.6 | 10.7 | 5.3 | 5.4 | 4.9 | 19.5 | 19.7 | 19.0 | 2.8 | 1.9 | 1.7 | 1 |
| Tm[4] | 1.07 | 1.3 | 1.77 | 2.5 | 1.8 | 0.8 | 0.8 | 0.9 | 3.7 | 3.2 | 3.1 | 0.5 | 0.4 | 0.3 | 0.1 |
| Yb[4] | 7.31 | 8.56 | 15 | 27.9 | 14.8 | 4.8 | 5.8 | 6.8 | 4.6 | 20.8 | 21.4 | 3.2 | 3.1 | 1.6 | 0.8 |
| Lu[4] | 1.05 | 1.23 | 2.3 | 4.43 | 2.19 | 0.7 | 0.9 | 1.1 | 4.4 | 3 | 3.1 | 0.5 | 0.5 | 0.2 | 0.13 |

Samples 1A/IH/2001, 2A/IH/2001, and 5/IH/2001 analyzed by Activation Laboratories (Canada), all other by X-ray Assay Laboratories (Canada). Analytical methods denoted by superscript codes as follows: [1]XRF, [2]ICP, [3]NA, [4]ICP-MS, [W]wet chemical; na—not analyzed. SMN-A1097 from Rämö (1991), analyses of Shachang granites from Yu et al. (1996a), analyses of Gross Spitzkoppe granites from Frindt et al. (2004a). Abbreviations for the plutons of the Newberry Mountains: SM–Spirit Mountain; M–Mirage; WRW–White Rock Wash.

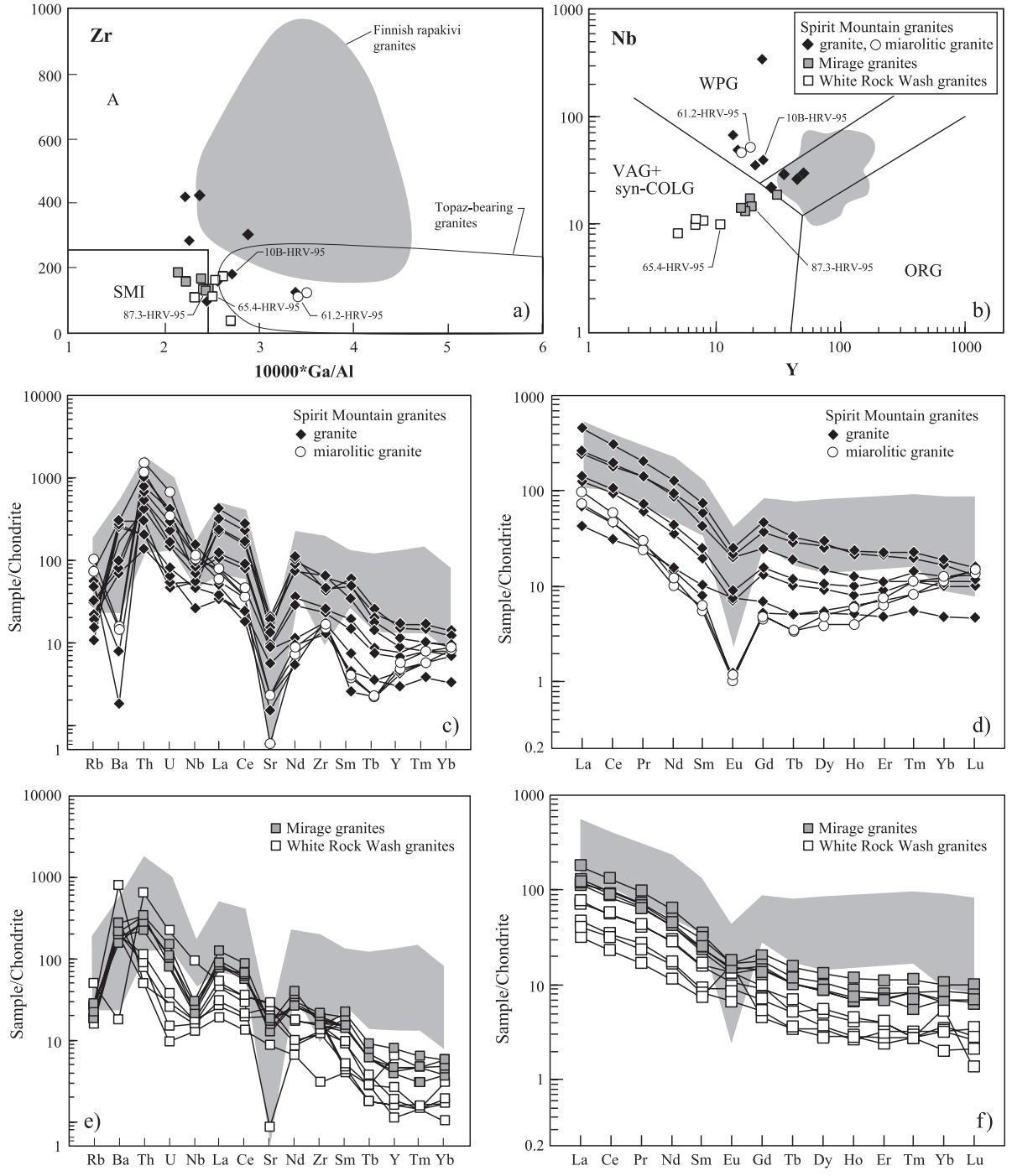



Fig. 14. Analyses of the granites of the Spirit Mountain pluton, Mirage pluton, and White Rock Wash pluton plotted in (a) Zr versus 10,000 Ga/Al (Whalen et al., 1987) and (b) Nb versus Y diagrams (Pearce et al., 1984); representative samples (Table 1) are indicated. Granites of the Spirit Mountain pluton (c and d) and granites of the Mirage and White Rock Wash plutons (e and f) are plotted separately on chondrite-normalized multielement spidergrams (c and e) and REE diagrams (d and f), respectively. The fields of the Finnish rapakivi granites (Fig. 3, shadowed) are indicated.

Table 2
Summary of Nd isotope data on the Spirit Mountain pluton, Newberry Mountains, southern Nevada (unpublished data by the authors)

| Sample | Rock type | $\varepsilon_{Nd}$ (at 15 Ma) | $T_{DM}$[a] |
|---|---|---|---|
| *Spirit mountain pluton* | | | |
| 3-HRV-92 | Granite | −9.6 | 1138 |
| 10B-HRV-92 | Granite | −10.1 | 1228 |
| 14-HRV-93 | Leucogranite | −9.6 | 1178 |
| 15A-HRV-93 | Granite | −10.2 | 1231 |
| 15D-HRV-93 | Rhyolite | −9.8 | 1034 |
| *Mirage pluton* | | | |
| 4.2-HRV-95 | Granite | −14.2 | 1491 |
| 14.3-HRV-95 | Granite | −14.2 | 1512 |
| 87.2-HRV-96 | Granite | −11.4 | 1338 |
| 28.1-HRV-95 | Diorite | −8.1 | 1317 |
| *White Rock Wash pluton* | | | |
| 65.4-HRV-95 | Two-mica granite | −16.1 | 1698 |
| 65.5-HRV-95 | Two-mica granite | −16.5 | 1884 |
| 73.1-HRV-95 | Two-mica granite | −16.3 | 1812 |
| 73.4-HRV-95 | Two-mica granite | −15.7 | 1670 |
| *Mafic dikes* | | | |
| 10-HRV-93 | Diabase | −4.1 | 946 |
| 11D-HRV-93 | Diabase | −8.4 | 1118 |
| 86.1-HRV-96 | Diabase | 0.0 | 992 |
| *Country rocks* | | | |
| 1-HRV-92 | Precambrian granite | −19.3 (−3.1)[b] | 2028 |
| 11-HRV-92 | Precambrian gneiss | −22.4 (−2.9)[b] | 1924 |

[a] Calculated according to the model of DePaolo (1981).
[b] Values in parenthesis calculated at 1450 Ma.

The isotopic and other geochemical data indicate different sources for the two Miocene extension-related granite plutons. SMP may have had both Mesozoic and Proterozoic felsic-intermediate crustal source components with some juvenile input, whereas MP has older (mainly Proterozoic) and probably more calcic average source. Falkner et al. (1995) reported for the granite of the Miocene Aztec Wash pluton from the adjacent Eldorado Mountains isotopic values, which are nearly identical with the SMP granites: $\varepsilon_{Nd}$ (at 15.7 Ma) of −10.1, Sr initial ratios of 0.7101 and 0.7102. The two granite plutons (SMP and Aztec Wash) obviously had remarkably similar sources and petrogenetic histories. Magmatic underplating or intraplating and partial melting of lower or middle crust is the preferred genetic model. The isotopic composition of the SMP granites suggests a mixed source—either the melted crust was previously hybridized or the mantle-derived magma and crustal magma interacted to form the hybrid magma. For the granites of the Eldorado Mountains, a similar conclusion was presented by Miller and Miller (2002).

## 6. Concluding remarks

The four described granitic associations from Finland and adjacent Fennoscandia, China, Namibia, and Nevada represent intracontinental magmatism that ranges in age from 1700 to 15 Ma. They are spatially and temporally far from each other but show many striking similarities, allowing some common petrogenetic interpretations.

1. In all four cases, the tectonic setting during granite emplacement was extensional, but the rocks represent different geotectonic environments. In the case of the rapakivi granites of Finland and adjacent Fennoscandia (age range 1670–1470 Ma, four area-constrained age groups), the magmatism was probably associated with long-lasting, large-scale mantle upwelling and incipient, aborted rifting. In China, the rapakivi magmatism had a short age span (1700–1680 Ma) and was associated with aborted rifting in the Archean North China craton. In Namibia, the anorogenic magmatism (137–123 Ma) was related to a mantle plume and "early" stages of continental rifting, which has continued as oceanic rifting. In the Basin and Range Province of Nevada and vicinity, 20–15 Ma rifting and related magmatism followed Mesozoic–early Tertiary subduction-related orogenic processes.
2. The magmatic association is in all cases bimodal. The silicic members are represented by granites and rhyolitic-quartz latitic dikes, the mafic members by gabbroic rocks and diabase dikes, and locally (Namibia) alkaline rocks. Intermediate rocks are relatively rare. Local magma mingling and hybridization are present in all case areas.
3. The granites show the chemical and mineralogical characteristics of within-plate granites and A-type granites. In the Newberry Mountains of southern

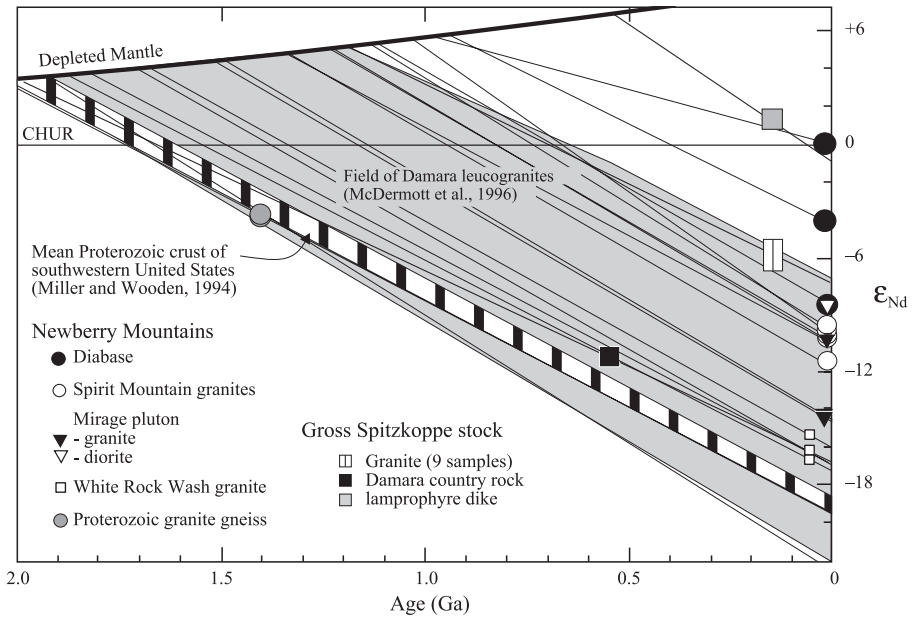



Fig. 15. $\varepsilon_{Nd}$ versus age diagram showing initial Nd isotope composition of the granites and associated rocks of the 125 Ma Gross Spitzkoppe stock in Namibia (Frindt, 2002) and the Newberry Mountains in southern Nevada (Haapala et al., 1996; Rämö et al., 1999). The $\varepsilon_{Nd}$ values were calculated for the Gross Spitzkoppe granites and a lamprophyre dike at 125 Ma, for the country rock (Damara granite) at 450 Ma, and for the rocks of the Newberry Mountains as follows: Spirit Mountain granites at 20 Ma, Mirage and diorite at 15 Ma, White Rock Wash granites at 65 Ma, diabase dikes at 15 Ma, Proterozoic granite gneiss at 1400 Ma. The shaded band shows the evolution of the Damara leucogranites in Namibia according to McDermott et al. (1996). The striped path shows the evolution of mean Proterozoic crust of the southwestern United States according to Miller and Wooden (1994). The thin lines show the evolution trends of individual samples. Evolution line of undifferentiated Earth (CHUR) is from DePaolo and Wasserburg (1976) and that of depleted mantle from DePaolo (1981).

Nevada, only the Spirit Mountain pluton shows clear within-plate character, however. In all four regions, the most evolved silicic members are topaz-bearing granites and rhyolites, and Sn–Be–W mineralization is in many cases associated with them.

4. Isotopic and geochemical studies suggest a prevailingly intermediate-felsic crustal source for the granites. Associated mafic rocks of all regions frequently have Nd isotope signatures largely overlapping with those of the associated granites. In some cases, however, some of the diabase dikes or basalts show chondritic or depleted mantle compositions [in Namibia $\varepsilon_{Nd}$ (at 125 Ma) up to +6], suggesting an asthenospheric mantle source. The composition of the mafic magmas was changed by assimilation of crustal rocks.
5. Magmatic underplating with voluminous dehydration partial melting of the deep crust is the most plausible mechanism for the bimodal magmatic association in all four cases. It explains the observed structural features of the lithosphere (thinning of the lower crust above mantle diapirs) as well as the geochemical and isotopic characteristics of the bimodal suites. The observed mantle component in the granites is probably related to mixing of the mantle-derived mafic magmas and crust-derived felsic magmas, or to anatectic melting of hybridized lower crust.
6. The reason for the mantle melting is not known in detail, and may also vary from one area to another. There is good evidence (e.g., isotopic and geochemical studies indicating depleted or near-chondritic mantle source) that in Namibia the Cretaceous anorogenic bimodal magmatism was caused by a deep mantle plume; it is not impossible that mantle plumes played a role in other areas as well. In the case of the Fenno-scandian rapakivi granites, partial melting of the

mantle material was possibly caused by thick crust that thermally insulated the underlying subcontinental mantle. This caused heating and large-scale upwelling of the solid mantle, eventually leading to magmatic underplating and partial melting. Mantle diapirism and associated extensive partial melting and reorganization of the crust stabilized the lithosphere in one area, and subsequent mantle diapirism appeared in neighboring area, being controlled by the heat flow in the mantle and the strength of the crust. In the case of the Colorado River extensional corridor (Basin and Range Province), the bimodal magmatism was largely synextensional, but opinions differ whether the strong extension (decompression) was the cause or the effect of the mantle magmatism.

## Acknowledgments

This report is based on long-term petrologic, geochemical, and isotopic research made by the rapakivi granite group of the University of Helsinki since the mid-1980s on anorogenic granitic magmatism in Finland, China, Namibia, and Nevada. Throughout the research, the authors have received support from several quarters, which is gratefully acknowledged. The results from the different areas have already been largely published, and this article has the character of a synthesizing review. During the fieldwork in China (1990, 1992), I.H. had fruitful cooperation with Professor Yu, Jianhua, Ms. Fu, Huiqin, Mr. Zhang, Fenglan, and Mr. Wan, Fangxiao, all from the Geological Institute of Beijing. In 1994–2002, S.F. and I.H. received important logistic and personal support from the Geological Survey of Namibia and the Geological Survey of Finland that had a joint mapping project in Damaraland in the1990s. The Master's theses of S.F. (Gross Spitzkoppe) and John Kandara (Klein Spitzkoppe) were done in the framework of this project. In southern Nevada, Professor Alex Volborth who had mapped the Newberry Mountains area in the 1960s, guided I.H. and O.T.R. in the field in southern Nevada in 1992. His later visits to the field, as well as his and Nadja von Volborth's hospitality, made our field research periods as pleasant as possible, the latest unforgettable one was in 2001. Isotope geological research has been an essential part of our studies. O.T.R. has had the privilege to use the isotope laboratory facilities of the Geological Survey of Finland since 1987—support and help from Drs. Hannu Huhma and Matti Vaasjoki in particular are warmly acknowledged. The manuscript was reviewed by Professors Eric H. Christiansen and Roberto Dall'Agnol, their suggestions and corrections improved the text markedly. Our studies have acquired financial support from Academy of Finland (Projects 36002 and 4067), the University of Helsinki, and the Centre of International Mobility (CIMO).

## References

Åhäll, K.I., Connelly, J.N., Brewer, T.S., 2000. Episodic rapakivi magmatism due to distal orogenesis? Correlation of 1.69–1.50 Ga orogenic and inboard, "anorogenic" events in the Baltic Shield. Geology 28, 823–826.

Ahl, M., Andersson, U.B., Lundqvist, T., Sundblad, K. (Eds.), 1997. Rapakivi Granites and Related Rocks in Central Sweden. Ser. Ca, vol. 87. pp. 1–99.

Alapieti, T., 1982. The Koillismaa layered igneous complex, Finland—its structure, mineralogy and geochemistry, with emphasis on the distribution of chromium. Bulletin-Geological Survey of Finland 319. 116 pp.

Alviola, R., Johanson, B.S., Rämö, O.T., Vaasjoki, M., 1999. The Proterozoic Ahvenisto rapakivi granite-massif-type anorthosite complex, southeastern Finland; Petrography and U–Pb chronology. In: Haapala, I., Rämö, O.T. (Eds.), Rapakivi Granites and Related Rocks. Precambrian Research, vol. 95. pp. 89–107.

Amelin, Yu., Larin, A.M., Tucker, R.D., 1997. Chronology of multiphase emplacement of the Salmi rapakivi granite–anorthosite complex, Baltic Shield: implications for magmatic evolution. Contributions to Mineralogy and Petrology 127, 348–368.

Anderson, J.L., Bender, E.E., 1989. Nature and origin of Proterozoic A-type granitic magmatism in the southwestern United States of America. Lithos 23, 19–52.

Andersson, U.B., 1997. Petrogenesis of some Proterozoic granitoid suites and associated basic rocks in Sweden geochemistry and isotope geology. Rapporter och Meddelanden-Sveriges Geologiska Undersökning 9. 213 pp.

Andersson, U.B., Neymark, L.A., Billström, K., 2002. Petrogenesis of the Mesoproterozoic (Subjotnian) rapakivi complexes of central Sweden: implications from U–Pb zircon ages, Nd, Sr and Pb isotopes. Transactions of the Royal Society of Edinburgh. Earth Sciences 92, 201–228.

Bridgewater, D., Sutton, J., Watterson, J., 1974. Crustal downfolding associated with igneous activity. Tectonophysics 21, 57–77.

Calzia, J.P., 1994. Petrogenesis of the middle Miocene rapakivi granite, Death Valley, California, USA. International Minera-

logical Association 16th General Meeting, Pisa. p. 62. Abstract volume.

Calzia, J.P., Rämö, O.T., 2000. Late Cenozoic crustal extension and magmatism, southern Death Valley region, California. In: Lageson, D.R., Peters, S.G., Lahren, M.M. (Eds.), Great Basin and Sierra Nevada. Field Guide-Geological Society of America, vol. 2. pp. 135–164.

Christiansen, E.H., Sheridan, M.F., Burt, D.M., 1986. The geology and geochemistry of the Cenozoic topaz rhyolites from the western United States. Special Paper-Geological Society of America 205. 82 pp.

Claesson, S., Kresten, P., 1997. The anorogenic Noran intrusion—a Mesoproterozoic rapakivi massif in south-central Sweden. Geologiska Foreningens i Stockholm Forhandlingar 119, 115–122.

Coney, P.J., 1987. The regional tectonic setting and possible causes of Cenozoic extension in North America Cordillera. In: Coward, M.P., Dewy, J.F., Hancock, P.L. (Eds.), Continental Extensional Tectonics. Special Publication-Geological Society of London, vol. 28. pp. 177–186.

Congdon, R.D., Nash, W.P., 1991. Eruptive pegmatite magma: rhyolite of the Honeycomb Hills, Utah. American Mineralogist 76, 1261–1278.

D'Andrea Kapp, J., Miller, C.F., Miller, J.S., 2002. Ireteba Pluton, Eldorado Mountains, Nevada: late, deep-source, peraluminous magmatism in the Cordilleran Interior. Journal of Geology 2002, 649–669.

DePaolo, D.J., 1981. Neodymium isotopes in the Colorado Front Range and crust–mantle evolution in the Proterozoic. Nature 291, 193–196.

DePaolo, D.J., Wasserburg, G.J., 1976. Nd isotopic variations and petrogenetic models. Geophysical Research Letters 3, 249–252.

Downes, H., Peltonen, P., Mänttäri, I., Sharkov, E.V., 2002. Proterozoic zircon ages from lower crustal granulite xenoliths, Kola Peninsula, Russia: evidence for crustal growth and reworking. Journal of the Geological Society (London) 159, 485–488.

Edén, P., 1991. A specialized topaz-bearing rapakivi granite and associated mineralized greisen in the Ahvenisto complex, SE Finland. Bulletin of the Geological Society of Finland 63, 25–40.

Eklund, O., Fröjdö, S., Lindberg, B., 1994. Magma mixing, the petrogenetic link between anorthositic suites and rapakivi granites, Åland, SW Finland. Mineralogy and Petrology 50, 3–19.

Eklund, O., Konopelko, D., Rutanen, H., Frõjdõ, S., Shebanov, A., 1998. 1.8 Ga Svecofennian post-collisional shoshonitic magmatism in the Fennoscandian shield. Lithos 45, 87–108.

Elliott, B.A., 2003. Petrogenesis of the postkinematic magmatism of the Central Finland Granitoid Complex II; sources and magmatic evolution. Journal of Petrology 44, 1681–1701.

Elo, S., Korja, A., 1993. Geophysical interpretation of the crustal and upper mantle structure in the Wiborg rapakivi granite area, southeastern Finland. In: Gorbatschev, R. (Ed.), Baltic Shield, Special Volume. Precambrian Research, vol. 64. pp. 273–288.

Emslie, R.F., 1978. Anorthosite massifs, rapakivi granites, and late Proterozoic rifting of North America. Precambrian Research 7, 61–98.

Emslie, R.F., Hamilton, M.A., Theriault, R.J., 1994. Petrogenesis of a Mid-Proterozoic anorthosite–mangerite–charnockite–granite (AMCG) complex: isotopic and chemical evidence from the Nain Plutonic Suite. Journal of Geology 102, 539–558.

Ewart, A., Milner, S.C., Armstrong, R.A., Duncan, A.R., 1998a. Etendeka volcanism of the Goboboseb Mountains and Messum Igneous Complex, Namibia: Part I. Geochemical evidence of early Cretaceous Tristan Plume melts and the role of crustal contamination in the Paraná-Etendeka CFB. Journal of Petrology 39, 191–225.

Ewart, A., Milner, S.C., Armstrong, R.A., Duncan, A.R., 1998b. Etendeka volcanism of the Goboboseb Mountains and Messum Igneous Complex, Namibia: Part II. Voluminous quartz latite volcanism of the Awahab magma system. Journal of Petrology 39, 227–253.

Falkner, C.M., Miller, C.F., Wooden, J.L., Heizler, M.T., 1995. Petrogenesis and tectonic significance of the calc-alkaline, bimodal Aztec Wash pluton, Eldorado Mountains, Colorado River extensional corridor. Journal of Geophysical Research 100, 10453–10476.

Frindt, S., 2002. Petrology of the Cretaceous anorogenic Gross Spitzkoppe granite stock, Namibia. PhD thesis, Department of Geology, University of Helsinki, Finland.

Frindt, S., Haapala, I., 2002. The Cretaceous Gross Spizkoppe granite stock in Namibia, a highly evolved A-type granite with structures and textures demonstrating magma flow, undercooling and vapor saturation during crystallization. 11th Quadrennial IAGOD Symposium and Geocongress 2002. Windhoek Namibia, 22–26 July. Extended Abstract volume [CD-ROM].

Frindt, S., Haapala, I., 2004. Anorogenic Gross Spitzkoppe granite stock in central western Namibia: Part II. Structures and textures indicating crystallization from undercooled melt. American Mineralogist 89, 857–866.

Frindt, S., Poutiainen, M., 2002. *P–T* path fluid evolution in the Gross Spitzkoppe granite stock, Namibia. Bulletin of the Geological Society of Finland 74, 103–114.

Frindt, S., Haapala, I., Pakkanen, L., 2004a. Anorogenic Gross Spitzkoppe granite stock in central western Namibia: Part I. Petrology and geochemistry. American Mineralogist 89, 841–856.

Frindt, S., Trumbull, R.B., Romer, R.L., 2004. Petrogenesis of the Gross Spitzkoppe topaz granite, central western Namibia: a geochemical and Nd–Sr–Pb isotope study. Chemical Geology 206, 43–71.

Frost, C.D., Frost, B.R., 1997. Reduced rapakivi-type granites: the tholeiite connection. Geology 25, 647–650.

Frost, C.D., Frost, B.R., Chamberlain, K.R., Edwards, B.R., 1999. Petrogenesis of the 1.43 Ga Sherman batholith, SE Wyoming, USA: a reduced, rapakivi-type anorogenic granite. Journal of Petrology 40, 1771–1802.

Frost, C.D., Frost, B.R., Bell, J.M., Chamberlain, K.R., 2002. The relationship between A-type granites and residual magmas from anortosites: evidence from the northern Sherman batholith, Laramie Mountains, Wyoming, USA. Precambrian Research 119, 45–71.

Gans, P.B., Mahood, G.A., Schermer, E., 1989. Synextensional magmatism in the Basin and Range Province; a case study from

the eastern Great Basin. Special Paper-Geological Society of America 233. 53 pp.
Green, R.W.E., 1983. Seismic refraction observations in the Damara orogen and flanking craton and their bearing on deep seated processes in the orogen. Special Publication-Geological Society of South Africa 11, 267–355.
Haapala, I., 1977a. The controls of tin and related mineralizations in the rapakivi granite areas of southeastern Fennoscandia. Geologiska Foreningens i Stockholm Forhandlingar 99, 130–142.
Haapala, I., 1977b. Petrography and geochemistry of the Eurajoki stock, a rapakivi–granite complex with greisen-type mineralization in southwestern Finland. Bulletin-Geological Survey of Finland 286. 128 pp.
Haapala, I., 1985. Metallogeny of the Proterozoic rapakivi granites of Finland. In: Taylor, R.P., Strong, D.F. (Eds.), Granite-Related Mineral Deposits: Geology, Petrogenesis, and Tectonic Setting. Extended abstracts of Papers Presented at the Canadian Institute of Mining and Metallurgy Conference on Granite-Related Mineral Deposits. September 15–17, 1985, Halifax, Canada. pp. 123–131.
Haapala, I., 1989. Suomen rapakivigraniiteista. Rapakivi granites of Finland. Academica Scientiarum Fennica. Year Book 1988–1989, 135–140 (in Finnish with an English summary).
Haapala, I., 1995. Metallogeny of the rapakivi granites. Mineralogy and Petrology 54, 149–160.
Haapala, I., 1997. Magmatic and postmagmatic processes in tin-mineralized granites: topaz-bearing leucogranites in the Eurajoki rapakivi granite stock, Finland. Journal of Petrology 38, 1645–1659.
Haapala, I., Rämö, O.T., 1990. Petrogenesis of the rapakivi granites of Finland. In: Stein, H.J., Hannah, J.L. (Eds.), Ore-bearing Granite Systems: Petrogenesis and Mineralizing Processes. Special Paper-Geological Society of America, vol. 246. pp. 275–286.
Haapala, I., Rämö, O.T., 1992. Tectonic setting and origin of the Proterozoic rapakivi granites of southeastern Fennoscandia. Transactions of the Royal Society of Edinburgh. Earth Sciences 83, 165–171.
Haapala, I., Rämö, O.T., 1999. Rapakivi granites and related rocks: an introduction. Precambrian Research 95, 1–7.
Haapala, I., Rämö, O.T., Volborth, A., 1995. Miocene rapakivi-like granites of southern Newberry Mountains, Nevada, U.S.A: Comparison to the Proterozoic rapakivi granites of Finland. In: Brown, M., Niccoli, P.M. (Eds.), The origin of granites and related rocks; Third Hutton Symposium, Abstracts. U.S. Geological Survey Circular, vol. 1129. pp. 61–62.
Haapala, I., Rämö, O.T., Volborth, A., 1996. Petrogenesis of the Miocene granites of Newberry Mountains, Colorado River extensional corridor, southern Nevada. Abstracts with Programs-Geological Society of America 28, 458.
Hamilton, W., 1987. Crustal extension in the Basin and Range province, southwestern United States. In: Coward, M.P., Dewey, J.F., Hancock, P.L. (Eds.), Continental Extensional Tectonics. Special Publication-Geological Society of London, vol. 28. pp. 155–176.
Hildreth, W., Halliday, A.N., Christiansen, R.L., 1991. Isotopic and chemical evidence concerning the genesis and contamination of basaltic and rhyolitic magma beneath the Yellowstone Plateau volcanic field. Journal of Geology 32, 63–138.
Hodges, K.V., Walker, J.D., 1992. Extension in the Cretaceous Sevier orogen, North American Cordillera. Geological Society of America Bulletin 104, 560–569.
Hoffman, P.J., 1989. Speculations on Laurentia's first giga-year (2.0–1.0 Ga). Geology 17, 135–138.
Hölttä, P., Huhma, H., Mänttäri, I., Peltonen, P., Juhanoja, J., 2000. Petrology and geochemistry of mafic granulite xenoliths from the Lahtojoki kimberlite pipe, eastern Finland. Lithos 51, 109–133.
Howard, K.A., John, B.E., 1987. Crustal extension along rooted systems of imbricate low-angle faults: Colorado River extensional corridor, California and Arizona. In: Coward, M.P., Dewey, J.F., Hancock, P.L. (Eds.), Continental Tectonics. Special Publication-Geological Society of London, vol. 28. pp. 299–311.
Howard, K.A., John, B.E., Davis, G.A., Anderson, J.L., Gans, P.B., 1994. A guide to Miocene extension in the lower Colorado River region, Nevada, Arizona, and California. Open-File Report (United States Geological Survey), 94–246.
Huhma, H., 1986. Sm–Nd, U–Pb and Pb–Pb isotopic evidence for the origin of Early Proterozoic Svecokarelian crust in Finland. Bulletin-Geological Survey of Finland 337. 48 pp.
Huppert, H.E., Sparks, S.J., 1988. The generation of granitic magmas by intrusion of basalt into continental crust. Journal of Petrology 29, 599–624.
Ishihara, S., 1977. The magnetite-series and ilmenite-series granite rocks. Mining Geology 27, 293–305.
Karhu, J.A., Holland, H.D., 1996. Carbon isotopes and the rise of atmospheric oxygen. Geology 24, 867–870.
Kempton, P.D., Downes, H., Neymark, L.A., Wartho, J.A., Zartman, R.E., Sharkov, E.V., 2001. Garnet granulite xenoliths from the northern Baltic shield—0the underplated lower crust of a Palaeoproterozoic large igneous province? Journal of Petrology 42, 731–763.
King, P.L., White, A.J.R., Chappell, B.W., Allen, C.M., 1997. Characterization and origin of aluminous A-type granites from the Lachlan Fold Belt, southeastern Australia. Journal of Petrology 38, 371–391.
Korja, A., Heikkinen, P., 1995. Proterozoic extensional tectonics of the central Fennoscandian Shield: results of the Baltic and Bothnian Echoes from the Lithosphere experiment. Tectonics 14, 504–517.
Korja, K., Korja, T., Luosto, U., Heikkinen, P., 1993. Seismic and geoelectric evidence for collisional and extensional events in the Fennoscandian Shield—implications for Precambrian crustal evolution. Tectonophysics 219, 129–152.
Korja, A., Heikkinen, P., Aaro, S., 2001. Crustal structure of the northern Baltic Sea paleorift. Tectonophysics 331, 341–358.
Korsman, K., Korja, T., Pajunen, M., Virransalo, P., 1999. The GGT/SVEKA Transect: Structure and evolution of continental crust in the Paleoproterozoic Svecofennian Orogen in Finland. International Geology Review 41, 287–333.
Kosunen, P., 1999. The rapakivi granite plutons of Bodom and Obbnäs, southern Finland. Bulletin of the Geological Society of Finland 71, 275–304.
Kosunen, P.J., Rämö, O.T., Vaasjoki, M., 2004. Petrogenesis of the Bodom and Obbnäs rapakivi plutons, southern Finland:

reduced, aluminous A-type granites from variable sources. Journal of Petrology (in review).

Lauri, L., Mänttäri, I., 2002. The Kynsijärvi quartz alkali feldspar syenite, Koillismaa, eastern Finland—silicic magmatism associated with 2.44 Ga continental rifting. Precambrian Research 119, 121–140.

Lindberg, B., Bergman, L., 1993. Pre-Quaternary rocks of the Vehmaa map-sheet area. Geological map of Finland 1:100,000. Explanation to the maps of pre-Quaternary rocks, sheet 1042. Geological Survey of Finland, Espoo, Finland.

Lindh, A., 2001. Microgranular enclaves in the Nordingrå rapakivi granite, east central Sweden—the early rapakivi development. Neues Jahrbuch für Mineralogie Abhandlungen 176, 299–322.

Lindh, A., Johansson, I., 1996. Rapakivi granites of the Baltic Shield: the Nordingrå granite, its chemical variation and Sm–Nd isotope composition. Neues Jahrbuch fur Mineralogie. Abhandlungen 170, 291–312.

Liu, D.Y., Shen, Q.H., Zhang, Z.Q., Jahn, B.M., Auvray, B., 1990. Archean crustal evolution in China: U–Pb geochronology of the Qianxi Complex. Precambrian Research 14, 185–202.

Luosto, U., 1997. Structure of the Earth's crust in Fennoscandia as revealed from refractive and wide-angle reflection studies. Geophysica 33, 3–16.

Luosto, U., Tiira, T., Korhonen, H., Azel, I., Burmin, V., Buyanov, A., Kosminskaya, I., Ionkis, V., Sharov, N., 1990. Crust and upper mantle structures along the DSS Baltic profile in SE Finland. Geophysical Journal International 10, 89–110.

Martin, H., Mathias, M., Simpson, E.S.W., 1960. The Damaraland sub-volcanic ring complexes in South West Africa. Report of the International Geological Congress XXI Session, vol. 13, pp. 156–174.

McCarthy, I., Larkin, S.P., Fuis, G.S., Simpson, R.W., Howard, K.A., 1991. Anatomy of a metamorphic core complex: seismic refraction/wide-angle reflection profiling in southeastern California and western Arizona. Journal of Geophysical Research 26, 12259–12291.

McDermott, F., Hawkesworth, C.J., 1990. Intracrustal recycling and upper-crustal evolution: a case study from the Pan-African Damara mobile belt, central Namibia. Chemical Geology 83, 263–280.

McDermott, F., Harris, N.B.W., Hawkesworth, C.J., 1996. Geochemical constraints on crustal anatexis: a case study from the Pan-African granitoids of Namibia. Contributions to Mineralogy and Petrology 123, 406–423.

Miller, R.M., 1983. The Pan-African Damara Orogen of South West Africa/Namibia. Special Publication-Geological Society of South Africa 11, 431–515.

Miller, C.F., Barton, M.D., 1990. Phanerozoic plutonism in the Cordilleran interior, USA. Special Paper-Geological Society of America 241, 213–231.

Miller, C.F., Miller, J.S., 2002. Contrasting stratified plutons exposed in tilt blocks, Eldorado Mountains, Colorado River rift, NV, USA. Lithos 61, 209–224.

Miller, C.F., Wooden, J.L., 1994. Anatexis, hybridization and modification of ancient crust: Mesozoic plutonism in the Old Woman Mountains area, California. Lithos 32, 135–156.

Miller, C.F., D'Andrea, J.L., Ayers, J.C., Coath, C.D., Harrison, T.M., 1997. BSE imaging and ion probe geochronology of zircon and monazite from plutons of the Eldorado and Newberry Mountains, Nevada: age, inheritance, and subsolidus modification. EOS 78, F783.

Milner, S.C., le Roex, A.P., 1996. Isotope characteristics of the Okenyenya igneous complex northwestern Namibia: constraints on the composition of the early Tristan Plume and the origin of the Emi mantle component. Earth and Planetary Science Letters 141, 277–291.

Milner, S.C., le Roex, A.P., O'Conner, J.M., 1995. Age of the Mesozoic igneous rocks in northwestern Namibia and their relationship to continental breakup. Journal of the Geological Society (London) 152, 97–104.

Neymark, L.A., Yu, V., Larin, A.M., 1994. Pb–Nd–Sr isotopic constraints on the origin on the 1.54–1.56 Ga Salmi rapakivi granite–anorthosite batholith (Karelia, Russia). Mineralogy and Petrology 50, 173–194.

Nironen, M., 1997. The Svecofennian orogen: a tectonic model. Precambrian Research 86, 21–44.

Nironen, M., Elliott, B.A., Rämö, O.T., 2000. 1.88–1.87 Ga post kinematic intrusions of the Central Finland Granitoid Complex: a shift from C-type to A-type magmatism during lithospheric convergence. Lithos 53, 37–58.

Nurmi, P.A., Haapala, I., 1986. The Proterozoic granitoids of Finland: granite types, metallogeny and relation to crustal evolution. Bulletin of the Geological Society of Finland 58, 203–233.

O'Conner, J.M., le Roex, A.P., 1992. South Atlantic hotspot–plume systems: 1. Distribution of volcanism in time and space. Earth and Planetary Science Letters 113, 343–364.

Patchett, J., Kouvo, O., 1986. Origin of continental crust of 1.9–1.7 Ga age: Nd isotopes and U–Pb zircon ages in the Svecokarelian terrain of South Finland. Contributions to Mineralogy and Petrology 92, 1–12.

Pearce, J.A., Harris, N.B.W., Tindle, A.G., 1984. Trace element discrimination diagrams for the tectonic interpretation of granitic rocks. Journal of Petrology 25, 956–983.

Peccerillo, A., Barberio, M.R., Yirgu, G., Ayalev, D., Barbieri, M., Wu, T.W., 2003. Relationships between mafic and peralkaline silicic magmatism in continental rift settings: a petrological, geochemical and isotopic study of Gedemsa Volcano, Central Ethiopian Rift. Journal of Petrology 44, 2003–2032.

Peltonen, P., Mänttäri, I., 2001. An ion microprobe U–Th–Pb study of zircon xenocrysts from the Lahtojoki kimberlite pipe, eastern Finland. Bulletin of the Geological Society of Finland 73, 47–58.

Persson, A.I., 1999. Absolute (U–Pb) and relative age determinations of intrusive rocks in the Ragunda rapakivi complex, central Sweden. Precambrian Research 95, 109–127.

Pesonen, L.J., Mertanen, S., 2002. Paleomagnetic configuration of continents during the Proterozoic. Institute of Seismology, University of Helsinki, Report S-42, pp. 103–109.

Pesonen L.J., Korja, A., Hjelt, S.-E., 2000. Lithosphere 2000, a symposium on structure, composition and evolution of the lithosphere in Finland. Programme and extended abstracts. Institute of Seismology Report S-41.

Prave, A.R., 1996. Tale of three cratons: tectonostratiographic anatomy of the Damara orogen in northwestern Namibia and the assembly of Gondwana. Geology 24, 1115–1118.

Puura, V., Flodén, T., 1999. Rapakivi–granite–anorthosite magmatism—a way of thinning and stabilisation of the Svecofennian crust, Baltic Sea Basin. Tectonophysics 305, 75–92.

Rabinowitz, P.D., LaBrecque, J.L., 1979. The Mesozoic South Atlantic Ocean and evolution of its continental margins. Journal of Geophysical Research 84, 5973–6002.

Rämö, O.T., 1991. Petrogenesis of the Proterozoic rapakivi granites and related basic rocks of southeastern Fennoscandia: Nd and Pb isotopic and general geochemical constraints. Bulletin-Geological Survey of Finland 355. 161 pp.

Rämö, O.T., 2001. Isotopic composition of pyterlite in Vyborg (Viipuri), Wiborg batholith, Russia. Bulletin of the Geological Society of Finland 73, 111–115.

Rämö, O.T., Haapala, I., 1995. One hundred years of rapakivi granite. Mineralogy and Petrology 52, 129–185.

Rämö, O.T., Haapala, I., 1996. Rapakivi granite magmatism: a global review with emphasis on petrogenesis. In: Demaiffe, D. (Ed.), Petrology and Geochemistry of Magmatic Suites of Rocks in the Continental and Oceanic Crust. A volume dedicated to Jean Michot. Universite Libre de Bruxelles, Royal Museum for Central Africa, pp. 177–200.

Rämö, O.T., Korja, A., 2000. Mid-Proterozoic evolution of the Fennoscandian Shield. Extended abstract, 31st IGC, Rio de Janeiro, August 2000. Abstract volume [CD-ROM].

Rämö, O.T., Luukkonen, E.J., 2001. 2.4 Ga A-type granites of the Kainuu region, eastern Finland: characterization and tectonic significance. EUG XI. European Union of Geosciences, April 8th–12th, 2001, Strasbourg, France: abstract volume. European Union of Geosciences, Strasbourg, pp. 771.

Rämö, O.T., Haapala, I., Vaasjoki, M., Yu, J., Fu, H., 1995. The 1700 Ma Shachang complex, northeast China: Proterozoic rapakivi granite not associated with Paleoproterozoic orogenic crust. Geology 23, 815–818.

Rämö, O.T., Huhma, H., Kirs, J., 1996. Radiogenic isotopes of the Estonian and Latvian rapakivi granite suites: new data from the concealed Precambrian of the East European Craton. Precambrian Research 79, 209–226.

Rämö, O.T., Haapala, I.J., Volborth, A., 1999. Isotopic and general geochemical constraints on the origin of Tertiary granitic plutonism in the Newberry Mountains, Colorado River Extensional Corridor, Nevada. Abstracts with Programs-Geological Society of America 31 (6), A86.

Rämö, O.T, Korja, A., Haapala, I., Eklund, O., Fröjdö, S., Vaasjoki, M., 2000. Evolution of the Fennoscandian lithosphere in the mid-Proterozoic: the rapakivi magmatism. Institute of Seismology, University of Helsinki, Report S-41, pp. 129–136.

Rieder, M., Haapala, I., Povondra, P., 1996. Mineralogy of dark mica from the Wiborg rapakivi batholith, southeastern Finland. European Journal of Mineralogy 8, 593–605.

Salonsaari, P.T., 1995. Hybridization in the bimodal Jaala-Iitti complex and its petrogenetic relationship to rapakivi granites and associated mafic rocks of southeastern Finland. Bulletin of the Geological Society of Finland 67 (Part 1b). 104 pp.

Schmitt, A.K., Emmermann, R., Trumbull, R.B., Bühn, B., Henjes-Kunst, F., 2000. Petrogenesis and $^{40}Ar/^{39}Ar$ geochronology of the Brandberg complex, Namibia: evidense for major mantle contribution in metaluminous and peralkaline granites. Journal of Petrology 41, 1207–1239.

Scott, R.B., Unruh, D.M., Snee, L.W., Harding, A.E., Nealey, L.D., Blank Jr., H.R., Budahn, J.R., Mehnert, H.H., 1995. Relation of peralkaline magmatism to heterogeneous extension during the middle Miocene, southeastern Nevada. Journal of Geophysical Research 100, 10381–10401.

Seth, B., Kröner, A., Mezger, K., Nemchin, A., Pidgeon, R.T., Okrusch, M., 1998. Archean to Neoproterozoic magmatic events in the Kaoko belt of NW Namibia and their geodynamic significance. Precambrian Research 92, 341–363.

Simonen, A., Vorma, A., 1969. Amphibole and biotite from rapakivi. Bulletin de la Commission Geologique de Finlande 238. 28 pp.

Suominen, V., 1991. The chronostratigraphy of southwestern Finland with special reference to Postjotnian and Subjotnian diabases. Bulletin-Geological Survey of Finland 356. 100 pp.

Taylor, R.P., 1992. Petrological and geochemical characteristics of the Pleasant Ridge zinnwaldite–topaz granite, south New Brunswick, and comparisons with other topaz-bearing felsic rocks. Canadian Mineralogist 30, 895–921.

Trumbull, R.B., Emmermann, R., Bühn, B., Gerstenberger, H., Mingram, B., Schmitt, A., Volker, F., 2000. Insight on the genesis of the Cretaceous Damaraland igneous complexes in Namibia from a Nd- and Sr-isotopic perspective. Communications of the Geological Survey of Namibia 12, 313–325.

Vaasjoki, M., Rämö, O.T., Sakko, M., 1991. New U–Pb ages from the Wiborg rapakivi area: constraints on the temporal evolution of the rapakivi granite–anorthosite–diabase dyke association of southeastern Finland. Precambrian Research 51, 227–243.

Volborth, A., 1973. Geology of the granite complex of the Eldorado, Newberry, and northern Dead Mountains, Clark County, Nevada. Bulletin-Nevada Bureau of Mines and Geology 80. 40 pp.

Vorma, A., 1976. On the petrochemistry of rapakivi granites with special reference to the Laitila massif, southwestern Finland. Bulletin-Geological Survey of Finland 285. 98 pp.

Wang, K., Windley, B.F., Sills, J.D., Yan, Y., 1990. The Archean gneiss complex in E. Hebei Province, north China: geochemistry and evolution. Precambrian Research 48, 245–265.

Welin, E., Christansson, K., Kähr, A.-M., 1993. Isotopic investigations of metasedimentary and igneous rocks in the Palaeoproterozoic Bothnian Basin, central Sweden. Geologiska Foreningens i Stockholm Forhandlingar 115, 285–296.

Wernicke, B., 1985. Uniform-sense normal simple shear of the continental lithosphere. Canadian Journal of Earth Sciences 22, 108–125.

Whalen, J.B., Currie, K.L., Chappell, B.W., 1987. A-type granites; Geochemical characteristics, discrimination, and petrogenesis. Contributions to Mineralogy and Petrology 95, 407–419.

Whalen, J.B., Jenner, G.A., Longstaffe, F., Robert, F., Gariéty, C., 1996. Geochemical and isotopic (O, Nd, Pd and Sr) constraints on A-type granite petrogenesis based on the Topsails igneous

suit, Newfoundland Appalachians. Journal of Petrology 37, 1463–1489.

White, R., McKenzie, D., 1989. Magmatism at rift zones: the generation of volcanic continental margins and flood basalts. Journal of Geophysical Research 94, 7685–7729.

Windley, B.F., 1995. The Evolving Continents, 3rd edition. John Wiley & Sons, Chichester.

Yu, I., Fu, H., Wan, F., 1994. Petrogenesis of potassic alkaline volcanics associated with rapakivi granites in the Proterozoic rift of Beijing, China. Mineralogy and Petrology 50, 83–96.

Yu, J.H., Fu, H.Q., Zhang, F.L., Wan, F.X., Haapala, I., Ramo, O.T., Vaasjoki, M., 1996a. Anorogenic Rapakivi Granites and Related Rocks in the Northern of the North China Craton. China Science and Tecnology Press, Beijing. In Chinese with English summary on pp. 137–182.

Yu, I., Fu, H., Haapala, I., Rämö, O.T., Vaasjoki, M., Mortenson, J.K., 1996b. Paleoproterozoic anorogenic rapakivi granite–anorthosite suite in the north part of the North China Craton. Progress in Geology of China. (1993–1996)—Papers to 30th IGC. pp. 104–108.

Zandt, G., Myers, S.C., Wallace, T.C., 1995. Crust and mantle structure across the Basin and Range-Colorado Plateau boundary at 37°N latitude and implications for Cenozoic extensional mechanism. Journal of Geophysical Research 100, 10529–10548.